Multimodality Imaging Guidelines for Patients with Repaired Tetralogy of Fallot: A Report from the American Society of Echocardiography
Developed in Collaboration with the Society for Cardiovascular Magnetic Resonance and the Society for Pediatric Radiology

Anne Marie Valente, MD, FASE, Co-Chair, Stephen Cook, MD, Pierluigi Festa, MD, H. Helen Ko, BS, RDMS, RDCS, FASE, Rajesh Krishnamurthy, MD, Andrew M. Taylor, MD, Carole A. Warnes, MD, Jacqueline Kreutzer, MD, and Tal Geva, MD, FASE, Co-Chair, *Boston, Massachusetts; Pittsburgh, Pennsylvania; Massa, Italy; New York, New York; Houston, Texas, London, United Kingdom; Rochester, Minnesota*

TABLE OF CONTENTS

1. EXECUTIVE SUMMARY

Advances in the diagnosis and management of congenital heart disease (CHD) have led to a marked improvement in the survival of patients with tetralogy of Fallot (TOF). However, residual anatomic and hemodynamic abnormalities are common. As with other types of congenital and acquired heart diseases, diagnostic information in patients with repaired TOF can be obtained using a variety of diagnostic tools. The choice of when to perform echocardiography, cardiovascular magnetic resonance (CMR) imaging, computed tomography (CT), nuclear scintigraphy, diagnostic catheterization, or a combination of these diagnostic procedures is dictated by the clinical question(s) asked and by a host of factors related to the patient, the modality, and the clinical circumstances. The aims of this document are to describe the role of each diagnostic modality in the care of patients with repaired TOF and to provide guidelines for a multimodality approach that takes into account patient-related and modality-related considerations.

Goals of Imaging

The overarching goals of diagnostic imaging are to identify anatomic and functional abnormalities, assess their severity, and provide information that informs clinical decisions. A list of essential data elements required for optimal management is summarized in section 4.

Imaging Modalities

In the following sections, each of the imaging modalities used for the evaluation of patients with repaired TOF is reviewed, and the strengths, weaknesses, and clinical utility of each modality are discussed. Finally, we propose an integrated multimodality imaging approach in this group of patients.

Echocardiography. Two-dimensional (2D) and Doppler echocardiography allow the evaluation of many of the anatomic and hemodynamic abnormalities in patients with repaired TOF. This modality is relatively inexpensive, widely available, not associated with exposure to harmful ionizing radiation, and portable. Therefore, echocardiography is ideally suited for longitudinal follow-up in this group of patients. Important limitations of the modality include difficulties in visualizing certain parts of the right heart because of restricted acoustic windows and challenges in quantitative assessment of right ventricular (RV) size and function and valve regurgitation.

CMR. CMR is considered the reference standard for the quantification of RV size and function and pulmonary regurgitation (PR) in patients with repaired TOF. The modality is ideally suited for longitudinal follow-up in this population because it allows comprehensive assessment of cardiovascular morphology and physiology without most of the limitations that hinder alternative imaging modalities. CMR is used selectively during the first decade of life, assuming a routine role in older patients.

Cardiovascular CT. Advances in multidetector computed tomographic technology have led to improvements in both spatial and temporal resolutions. Multidetector CT (MDCT) is used in patients with repaired TOF in whom CMR is contraindicated or unavailable.

Nuclear Scintigraphy. In current practice, the primary use of nuclear imaging in patients with repaired TOF is to measure pulmonary perfusion.

X-Ray Angiography. Diagnostic cardiac catheterization is rarely used primarily for imaging purposes in patients with repaired TOF. However, it serves an important role when essential information cannot be accurately obtained noninvasively. Additionally, x-ray angiography is an integral component of catheter-based procedures such as pulmonary artery (PA) balloon dilation and stenting and percutaneous pulmonary valve (PV) implantation. In adult patients at risk for acquired coronary artery disease, coronary angiography may be indicated.

Multimodality Imaging

No single modality is able to delineate all aspects of the intracardiac and extracardiac anatomy, evaluate hemodynamic consequences of TOF repair, be cost effective, reach patients in various locations, not cause excessive discomfort and morbidity, and not expose patients to harmful effects of ionizing radiation. Therefore, a multimodality approach that takes into account patient-specific considerations, strengths and weaknesses of each modality, and institutional resources and expertise is recommended.

2. BACKGROUND

TOF is the most common cyanotic CHD, with an average incidence of 32.6 per 100,000 live births.[1] With an annual birth rate in the United States of approximately 4 million live births,[2] roughly 1,300 new patients with TOF are born each year. Advances in diagnosis and management of CHD have led to marked improvement in the survival of patients born with TOF. Contemporary reports indicate that >98% of these infants survive surgical repair of their cardiac anomaly, with repair usually performed during the first year of life.[3] Studies of long-term outcomes show a 30-year survival rate of 90%.[4] As a result of these demographic trends,

the number of patients with repaired TOF increases each year, and in many communities, adult survivors now outnumber infants and children.[5]

Despite major advances in intracardiac surgery since Lillehei and Varco reported the first TOF repair by an open-heart procedure in 1954, residual anatomic and hemodynamic abnormalities are nearly universal. In the majority of patients, relief of the RV outflow tract (RVOT) obstruction requires disruption of PV integrity, which leads to PR. Residual or recurrent RVOT obstruction can occur at any age but is more commonly encountered in the first several years after the initial repair. Surgical relief of the RVOT obstruction usually involves infundibulotomy, resection of obstructive muscle bundles, and the use of a patch to enlarge the pathway from the right ventricle to the PAs. These procedures result in scar tissue and a noncontracting RVOT free wall, which can progress to become an aneurysm. Branch PA stenosis, residual atrial septal defect or ventricular septal defect (VSD), tricuspid regurgitation (TR), RV dilatation and dysfunction, aortic dilatation, aortic regurgitation (AR), and left ventricular (LV) dysfunction are some of the anatomic and functional abnormalities encountered in patients with repaired TOF (Table 1). Conduction and rhythm abnormalities are another source of considerable morbidity and are associated with mortality in this patient population.[6] Right bundle branch block with prolongation of the QRS complex on surface electrocardiography is nearly universal; atrial flutter or fibrillation and ventricular tachycardia are seen with increasing frequency beginning in the third and fourth decades of life.[7]

Although the hemodynamic burden associated with these anomalies is often tolerated well during childhood and adolescence, the incidences of arrhythmias, exercise intolerance, heart failure, and death increase beginning in early adulthood.[7,8] Thus, the nearly universal anatomic and functional anomalies that characterize the cardiovascular system of patients with repaired TOF and the associated morbidities and ongoing risk for premature death provide the rationale for close lifelong medical surveillance. Diagnostic imaging is a mainstay of the evaluation in this patient population, providing clinicians with information on anatomic and hemodynamic abnormalities, including their locations, severity, and changes over time. This information is vital for informing clinical decisions such as when to recommend PV implantation and other transcatheter or surgical procedures.

As with other types of congenital and acquired heart diseases, diagnostic information in patients with repaired TOF can be obtained using a variety of diagnostic tools.[9-12] The choice of when to perform echocardiography, CMR imaging, CT, nuclear scintigraphy, diagnostic catheterization, or a combination of these diagnostic procedures is dictated by the clinical question(s) asked and by a host of factors related to the patient, the modality, and the clinical circumstances. The aims of this document are to describe the role of each diagnostic modality in the care of patients with repaired TOF and to provide guidelines for a multimodality approach that takes into account patient-related and modality-related considerations. For each imaging modality, we provide a general overview, discuss its strengths and weaknesses, and present guidelines for use of the modality in patients with repaired TOF.

The document focuses on patients with repaired TOF with pulmonary stenosis or atresia, including those with RVOT patches or conduits between the right ventricle and PAs. In less common anatomic and surgical scenarios (e.g., TOF with atrioventricular canal, TOF with discontinuous PAs and open VSD), the frequency and type of imaging tests should be further tailored to the patient's specific

Table 1 Structural and functional abnormalities encountered in repaired TOF (modified from Geva[11])

Structural abnormalities	Functional abnormalities
Inherent to TOF repair	RV volume overload
Partial or complete removal of PV tissue	PR
Infundibulotomy scar	TR
Resection of RV/infundibular muscle bundles	Left-to-right shunt
Right atriotomy scar	VSD
VSD patch	Atrial septal defect
Residual or recurrent lesions	Systemic-to-pulmonary collateral vessels
RVOT obstruction	RV pressure overload
Main or branch PA stenosis	RVOT or PA stenosis
VSD	Pulmonary vascular disease
Atrial septal defect	Pulmonary venous hypertension secondary to LV diastolic dysfunction
Acquired lesions	RV systolic dysfunction
TV abnormalities	RV diastolic dysfunction
RVOT aneurysm	LV dysfunction
RV fibrosis	AR
Associated anomalies	Ventricular conduction delay and dyssynchrony
Dilated aorta	Arrhythmias
Associated congenital cardiovascular anomalies	Atrial flutter
Associated genetic noncardiac anomalies	Atrial fibrillation
	Ventricular tachycardia
	Comorbidities
	Renal, pulmonary, musculoskeletal, neurodevelopmental abnormalities

circumstance. It is important to note that this document does not recommend management strategies for these patients but rather focuses on the optimal utilization of contemporary imaging modalities.

3. GENERAL CONSIDERATIONS

As with any patient with CHD, knowledge of the patient's prior medical and surgical histories is paramount to successful noninvasive diagnostic imaging. To that end, access to medical records, including operative reports, is invaluable. In the absence of such documentation, comprehensive review of the patient's history is helpful. In the occasional patient without an available history, surveillance of the chest wall for surgical scars (e.g., left or right thoracotomy vs sternotomy) can offer important clues suggestive of a palliative shunt versus definitive repair. The patient's age can also offer a hint as to whether a classic or a modified Blalock-Taussig shunt was performed (the latter became common practice in 1985).[13,14] History of a previous Blalock-Taussig shunt should prompt evaluation of the ipsilateral branch PA for tenting and stenosis at the shunt insertion site.[15] Similarly, knowledge of a previous Waterston shunt requires critical evaluation of the right PA (RPA), whereas a prior Potts shunt should prompt assessment of the left PA (LPA) for stenosis or a residual shunt.[16,17] In either shunt, the imager should be aware of the possibility of pulmonary hypertension due to vascular disease in the lung(s) supplied by the systemic-to-PA shunt.[18] Low oxygen saturation may be a sign of residual right-to-left shunt and should prompt a detailed evaluation for the source of the shunt.

Awareness of certain genetic syndromes may help further guide diagnostic imaging in patients with TOF.[19] For example, patients with TOF and pulmonary atresia as well as chromosome 22q11 deletion are prone to have crossed PAs, abnormal branching pattern of the brachiocephalic arteries, and a retroaortic innominate vein.[20,21]

4. GOALS OF IMAGING

In a patient with repaired TOF, each of the abnormalities listed in Table 1 should be evaluated periodically using a combination of imaging modalities. Recognizing that no single modality is capable of providing all the necessary data, and being cognizant of the importance of using resources judiciously, in-depth understanding of the strengths and weaknesses of each modality is vital to quality patient care.

The following is a list of data essential for optimal management of most patients with repaired TOF:

- RV size and function
- TR (degree and mechanism)
- RV pressure
- Regional RV wall motion abnormalities
- Evaluation of the RVOT for obstruction and/or aneurysm
- Assessment of the main and branch PAs
- Degree of PR
- LV size and function
- Size of the aortic root and ascending aorta
- Degree of AR
- Aortic arch sidedness
- Origin and proximal course of the left and right coronary arteries
- Presence of systemic-to-pulmonary collateral vessels
- Residual intracardiac and extracardiac shunts
- Assessment of myocardial viability
- Associated anomalies (e.g., anomalies of the systemic or pulmonary veins)

5. ECHOCARDIOGRAPHY

a. Overview of Modality

Two-dimensional and Doppler echocardiography allows the evaluation of many of the anatomic and hemodynamic abnormalities in

patients with repaired TOF. As detailed in subsequent sections, 2D imaging allows qualitative and quantitative assessments of the right atrium, right ventricle, RVOT, PAs, tricuspid valve (TV), PV, and atrial and ventricular septa. Given the potential for LV dysfunction, dilatation of the proximal aorta, and AR, assessment of the left heart is integral to the echocardiographic assessment of the patient with repaired TOF. Doppler echocardiography is particularly important in this population for noninvasive hemodynamic assessment of parameters such as RV and PA pressures. Three-dimensional (3D) echocardiography can further aid in delineating anatomic pathology and biventricular size and function. Transesophageal echocardiography (TEE) is useful in certain patients to guide interventional procedures or evaluate valve anatomy when transthoracic imaging is challenging or when infective endocarditis is suspected. More recently, the role of myocardial deformation imaging for assessment of RV function is a topic of intense investigation in this patient population.[22]

b. Strength and Limitations

Echocardiography is the primary noninvasive imaging modality in patients with CHD, including those with repaired TOF.[9,12] This modality is relatively inexpensive, widely available, portable, and not associated with exposure to harmful ionizing radiation. Importantly, experience with echocardiography is extensive, and clinicians caring for these patients are familiar with its application.

Important limitations of echocardiography in this group of patients include difficulties in visualizing certain parts of the right heart because of restricted acoustic windows and challenges in quantitative assessments of RV size and function and valve regurgitation. These limitations are usually of lesser concern during the first decade of life because the acoustic windows are not as restricted as in older patients with larger body sizes and because the majority of these patients tend to be clinically well. Once patients reach adolescence and adulthood, acoustic windows tend to become more challenging, and the importance of accurate quantitative assessment of RV size and function requires the complementary use of echocardiography and other modalities, most often CMR.

c. Assessment of Repaired TOF with Echocardiography

RVOT. In young patients with good subcostal windows, the RVOT can be evaluated in the long-axis and short-axis planes and in the inflow-outflow view, analogous to the angiographic right anterior oblique plane (transducer mark at 1–2 o'clock). In the great majority of patients, the RVOT can be thoroughly evaluated from the parasternal long-axis and short-axis views, which facilitates assessment of the infundibulum and any associated aneurysm, residual PV tissue, and main and branch PAs. The RVOT dimension at the site of the former PV is important when transcatheter valve implantation is being considered. Attention is paid to the presence of RV hypertrophy, which is defined in adults as RV diastolic wall thickness > 5 mm.[23] In most patients with repaired TOF, however, the infundibular free wall is composed of a patch, and its thickness might not reflect RV hypertrophy in other parts of the chamber.

When evaluating for residual RVOT obstruction, it is important to identify the site of obstruction using color, pulsed-wave, and continuous-wave Doppler. In the case of an RV-to-PA conduit, the obstruction can be at any location along the entire length of the conduit, with or without involvement of the origins of the PAs. The spectral Doppler flow profile across the RVOT can help differentiate between dynamic obstruction within the RV cavity and residual valvar or supravalvar stenosis. The former has late peaking of the

Doppler signal ("lobster claw" shape), whereas the latter has midsystolic peaking. In patients with normal cardiac output, a peak instantaneous gradient of >4 m/sec (>64 mm Hg) is considered severe stenosis, 3 to 4 m/sec (36–64 mm Hg) is considered moderate stenosis, and <3 m/sec (<36 mm Hg) is considered mild stenosis.[24]

Multiple levels of obstructions in the RVOT and PAs pose a particular challenge to differentiate the contribution at each level, especially when they are in close proximity. In older patients or in patients with RV-to-PA conduits, the branch PAs are sometimes difficult to assess for residual stenosis because of the high flow velocity within the conduit. A high TR jet velocity should prompt a careful search for RVOT or PA obstruction at some level.

PAs. The PAs are evaluated using a combination of 2D imaging and color and spectral Doppler. The suprasternal and high left and right parasternal windows are used to image the mediastinal PAs, although imaging may be challenging in patients with larger body habitus. The main PA (MPA) is measured at its midpoint during systole. When supravalvar PA stenosis is present, the smallest diameter is measured as well. The diameters of the branch PAs are measured at the level of the origin, and the smallest dimension of any stenotic segment should be reported. The subcostal long-axis, high left parasternal short-axis, suprasternal short-axis, and right parasternal short-axis views are helpful in visualizing the length of the RPA. The high left parasternal short-axis and the suprasternal long-axis (near parasagittal plane angled to the left) views are useful in visualizing the length of the LPA. The distal LPA is more difficult to image than the RPA because of interference from air in the lung and the left bronchus.

PR. PR, occurring as a result of transannular patching, pulmonary valvotomy or valvectomy, or any other procedure that disrupts the valve, is an important factor in the long-term outcomes of patients with repaired TOF.[25-27] It is a key initiating element in a pathophysiologic cascade that leads to RV dilatation and dysfunction, which in turn has been linked to secondary TR, decreased exercise capacity, and increased risk for atrial and ventricular arrhythmias, as well as sudden cardiac death.[28-30] Therefore, evaluation of PR is an essential component of the echocardiographic examination in these patients.

PR jets are easily visualized by color Doppler in the RVOT, especially when evaluated in the parasternal long-axis and short-axis planes.[31] It is worth noting that in the context of "wide open/free" PR, the jet(s) may be overlooked by color Doppler because the flow is laminar with low velocity. Validation studies of the severity of PR by echocardiography have compared Doppler parameters with the gold standard of CMR.[32-34] Predictors of severe PR by Doppler included diastolic flow reversal (either by color Doppler flow mapping or by spectral pulsed-wave Doppler) in the main or branch PAs coupled with a PR jet width on color Doppler ≥ 50% of the pulmonary annulus (Figure 1). Others have used a PR jet width/pulmonary annulus ratio cutoff of >0.7 to identify a CMR PR fraction ≥ 40%.[33,34] Short deceleration time in the PR spectral Doppler signal is usually indicative of severe PR and often leaves a long period of "no flow" or antegrade flow in the latter part of diastole. This spectral appearance relates to the rapid equilibration of PA and RV diastolic pressures. The duration of the PR signal in the spectral Doppler trace compared with the total duration of diastole has been called the PR index. A value < 0.77 has been shown to have high sensitivity and specificity for identifying patients with CMR-derived PR fractions > 25%, which can be viewed as "significant."[32] A pressure half-time < 100 msec has good sensitivity and
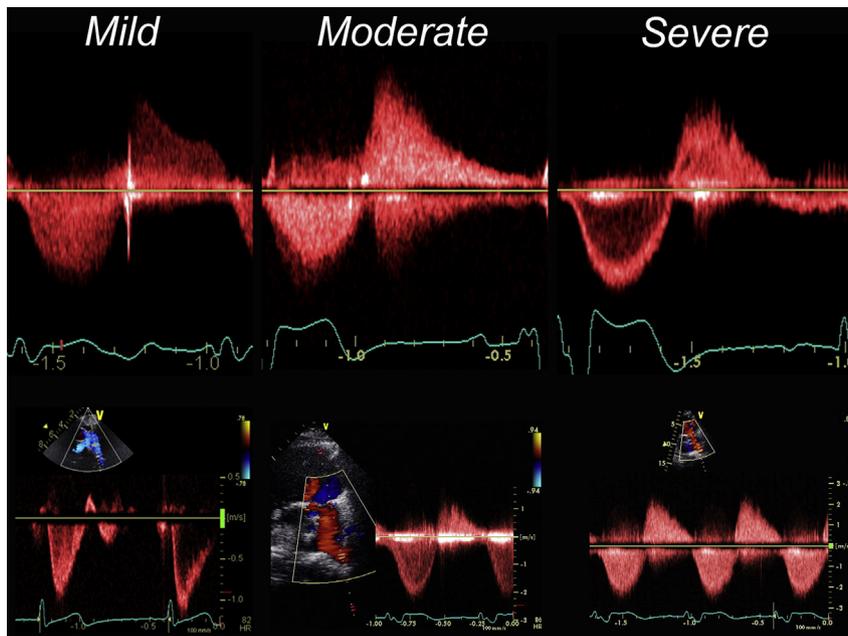
Figure 1 Evaluation of PR by Doppler echocardiography showing mild, moderate, and severe degrees. (*Top row*) Spectral Doppler tracing. Mild regurgitation is characterized by a persistent flow gradient at end-diastole and moderate regurgitation by equilibration of pressures between the MPA and right ventricle only at end-diastole, and severe regurgitation is associated with early diastolic pressure equilibration. (*Bottom row*) Pulse Doppler interrogation in the LPA showing degrees of diastolic flow reversal. See text for details.

specificity for severe PR.[35] It should be noted that this measurement might not be reliable in the presence of high RV end-diastolic pressure, which contributes to early pressure equilibration between the MPA and the right ventricle.

TV Morphology and Function. TR is commonly encountered in patients with repaired TOF and may be due to several factors. One mechanism involves disruption of the integrity of the tricuspid septal-anterior commissure by the VSD patch. This results in a TR jet originating at the junction between the VSD patch and the septal attachment of the TV and extending along the atrial septum (Figure 2). Other mechanisms include annular dilatation secondary to RV enlargement and basal-lateral displacement of the free wall papillary muscles. The latter also results from RV dilatation and altered chamber geometry that distorts the subvalvar apparatus. In addition, TR can result from damage secondary to a transvenous pacemaker or an implantable defibrillator or from bacterial endocarditis. Rarely, TR is due to intrinsic congenital abnormalities of the valve.

The mechanism of TR is determined by a combination of 2D, 3D, and color Doppler flow imaging. Simultaneous depiction of 2D and color Doppler flow imaging facilitates depiction of the TR jet relative to anatomic structures seen on 2D images. Three-dimensional imaging with en face views of the valve as seen from the right atrium and from the right ventricle can be particularly helpful when image quality and temporal resolutions are adequate. Measurements of the TV tethering height and area (Figure 3) have been shown in adult patients with functional TR and with pulmonary hypertension to provide insights into the mechanism of regurgitation.[36,37]

Unlike mitral regurgitation, there are limited data on TR quantification. Color Doppler in combination with the profile and intensity of the spectral Doppler signal are used for assessment of TR severity. The vena contracta width, regurgitant jet diameter, and intensity of the Doppler signal have all been related to the degree of regurgitation.
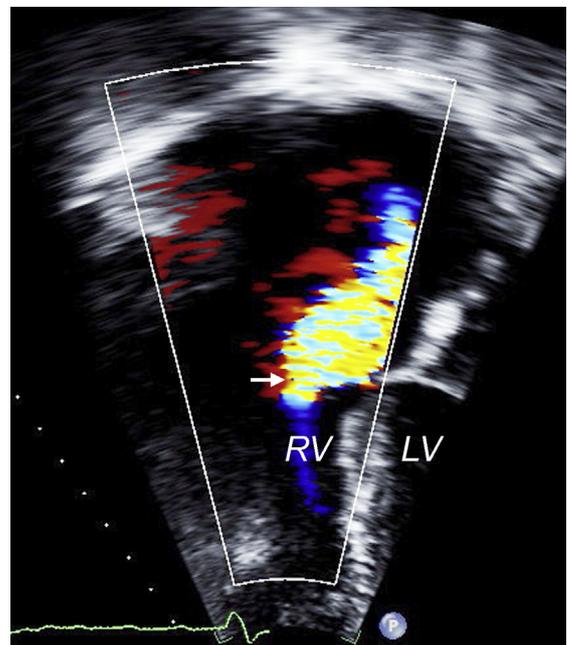
Figure 2 Moderate TR (*arrow*) due to impingement of the VSD patch on the septal-anterior commissure. *LV*, Left ventricle; *RV*, right ventricle.

It is important to note that with TV annular dilatation, the regurgitant jet needs to be assessed from multiple echocardiographic windows to minimize errors from underappreciating the regurgitation. In practice, the vena contracta width is the most reliable parameter to quantify TR. Zoghbi *et al.*[31] defined a vena contracta width > 0.7 cm as indicating severe TR. Both the proximal isovelocity surface area and vena contracta methods are reported to be more accurate for central
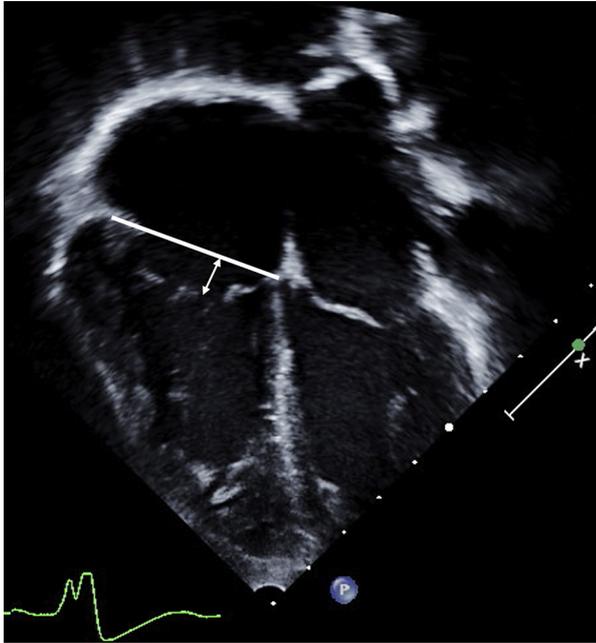
Figure 3 Apical four-chamber view (systolic frame) showing measurement of TV tethering height.

jets as opposed to eccentric jets. However, a 20% to 30% underestimation of TR severity can occur using the proximal isovelocity surface area or jet area method.[38] In practice, the proximal isovelocity surface area method is seldom used for TR severity. In addition to evaluating the TR jet by color Doppler and measuring the vena contracta width, the size of the inferior vena cava (IVC) and right atrium and hepatic venous flow reversal are used to assess TR severity. However, these indirect signs are also influenced by other factors, such as RV compliance, RV preload, and atrial tachyarrhythmias.

Right Ventricle. *i. Size.*–Challenges in determining RV size by echocardiography include its retrosternal position, highly variable geometry that does not conform to standard geometric models, and difficulties in imaging the entire chamber by 3D echocardiography in a significant number of patients. RV size is determined by 2D echocardiography from multiple acoustic windows.[23] The normally crescentic shape of the right ventricle is best appreciated in the short-axis view; if the right ventricle's short-axis anteroposterior (AP) diameter is larger than that of the left ventricle at the level of the papillary muscles, it is considered severely enlarged. The right ventricle is measured from an RV-focused apical four-chamber view with both the crux and the apex visible to avoid foreshortening. RV end-diastolic cross-sectional area < 20 cm^2/m^2 body surface area (BSA) has been associated with CMR-measured RV end-diastolic volume index < 170 mL/m^2.[39] A diameter > 42 mm at the base and > 35 mm at the midventricular level indicate RV dilatation.[23] Note that the latter cutoff values are not adjusted to body size.

ii. Function.–Although guidelines for assessment of RV size and function in adults are available,[23] only limited information exists on the accuracy, reproducibility, and prognostic value of these echocardiography-derived data in patients with repaired TOF. Nevertheless, a quantitative approach to assessment of RV size and function is preferred to qualitative assessment (the "eyeball method") because the latter has been shown to be inadequate.[40]

In general, 2D-based measurements correlate only modestly with CMR-derived RV volumes and ejection fraction (EF), and the degree of discrepancy increases as the right ventricle dilates.[41] Evidence suggests that compared with 2D-based measurements, 3D echocardiography provides more accurate and reproducible quantification of RV volumes.[23,42-46] However, a meta-analysis suggested that 3D echocardiography consistently underestimates RV volumes and EF,[47] a discrepancy that might increase as the right ventricle becomes severely enlarged.[44] However, only limited normative data are available to allow routine use of 3D echocardiography in the quantification of RV volumes and EF. In a study of 70 patients with a variety of CHDs undergoing transthoracic 3D echocardiography, Renella et al.[48] reported that RV volume and EF could not be measured in 42% because of technical limitations, mostly because of restricted acoustic windows and an inability to include the entire chamber within the 3D volume.

RV dilatation and dysfunction in patients with repaired TOF adversely affect LV geometry and function.[49] RV volume and pressure overload are associated with flattening or leftward displacement of the intraventricular septum, which results in a D-shaped left ventricle, which can interfere with diastolic filling. *Ventricular-ventricular interaction* is a term that has been used to describe the association between worsening RV dilatation and dysfunction and declining LV systolic function.[50,51] Factors contributing to this phenomenon include the above-mentioned geometric remodeling, shared myofibers, and a shared pericardial space.[11] Furthermore, the pathophysiology of the right ventricle after TOF repair is associated with impaired electromechanical synchrony, which affects global biventricular function.[52,53]

The percentage RV fractional area change is a measure of RV systolic function and is defined as ([end-diastolic area $-$ end-systolic area]/end-diastolic area) $\times$ 100. The RV endocardium is traced in systole (minimal area) and end-diastole (maximal area), as shown in Figure 4. Care must be taken to trace the endocardium beneath the trabeculations along the free wall. The lower reference value for normal RV systolic function using this method is 35%. This value correlates modestly with CMR measurements in patients with CHD.[54,55] In patients with repaired TOF, studies have shown low to modest correlations between RV fractional area change and CMR-derived RV EF.[41,56]

Nongeometric methods used to evaluate RV function include the rate of pressure rise in the right ventricle (dP/dt),[57] myocardial acceleration during isovolumic contraction,[58-60] and the Tei index[61] (also known as the myocardial performance index). However, the clinical utility of these parameters in patients with repaired TOF is unclear.[62-65]

Another method of measuring longitudinal RV function is the tricuspid annular motion or the tricuspid annular plane systolic excursion (TAPSE). This parameter measures the excursion distance of the lateral TV annulus during systole from the apical four-chamber window (Figure 5). The measurement can be obtained by M-mode or 2D imaging. The assumption that underlies this parameter is that it reflects global RV function, which may not be the case in patients with repaired TOF. Studies in non-CHD patients have reported a modest correlation between TAPSE and CMR-derived RV EF.[66-68] Importantly, in patients with repaired TOF, the correlations between TAPSE and CMR-derived RV EF and RV end-diastolic volume index are weak.[56,69-71] American Society of Echocardiography (ASE) guidelines indicate TAPSE of 16 mm as the lower limit of normal RV systolic function in adult patients. Koestenberger et al.[72] reported TAPSE values in 640 healthy children and demonstrated that TAPSE had a positive nonlinear relationship with age and BSA,
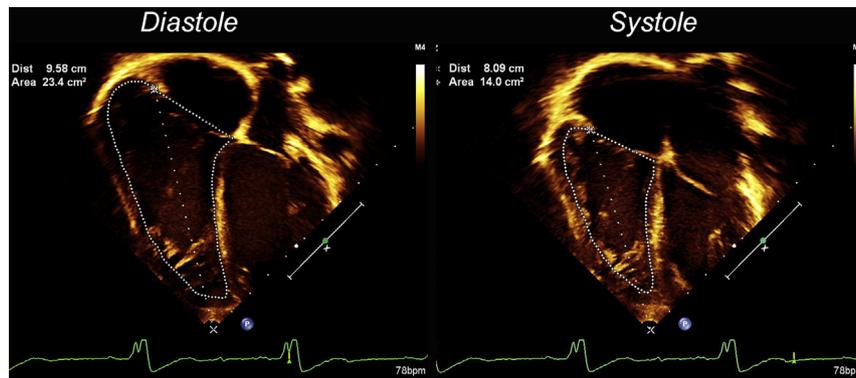
Figure 4 Evaluation of RV size and function using the fractional area change method. Note that apical transducer position is optimized to image the right ventricle.
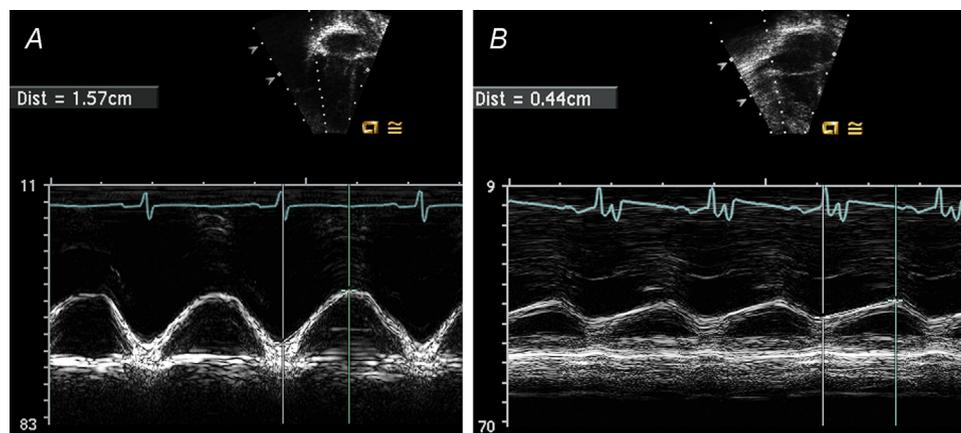
Figure 5 TAPSE of **(A)** normal and **(B)** depressed RV systolic function.

ranging from a mean of 9.1 mm in neonates to 24.7 mm in 18-year-old subjects.

Tissue Doppler (Figure 6) allows analysis of the velocity of the longitudinal motion of the tricuspid annulus as well as the RV basal free wall (RV S' or RV systolic excursion velocity). Both pulsed tissue Doppler and color-coded tissue Doppler can be used. However, it should be noted that the peak velocity obtained by pulsed tissue Doppler tends to be higher than the velocity attained by color-coded tissue Doppler, which represents mean velocity. The ASE guidelines state that an S' < 10 cm/sec by pulsed tissue Doppler suggests RV dysfunction.[23] No specific guideline for color-coded tissue Doppler analysis is available. A reference range for RV S' derived from 860 healthy children revealed a mean of 7.2 cm/sec in newborns to 14.3 cm/sec in 18-year-old individuals. Despite a significant positive correlation with age and BSA, the study reported a low correlation between S' and TAPSE.[73] Pavlicek et al.[74] reported that S' < 11cm/sec best detected a CMR-derived RV EF < 50% in 223 subjects, 13% of whom had repaired TOF. Kutty et al.[75] divided the right ventricle into the sinus portion and the outflow tract to evaluate the effect of regional dysfunction on tissue Doppler assessment of global RV systolic function assessed by CMR. They found that compared with patients with severe RVOT dysfunction (infundibular EF < 30%), those with infundibular EFs ≥ 30% had a better correlation between S' and global RV EF.

Echocardiographic assessment of myocardial deformation has attracted substantial interest in recent years. Parameters such as myocardial strain and strain rate are measured by color-coded tissue Doppler or 2D speckle-tracking. Because of the lack of an industry standard, it is difficult to assess these technologies across different platforms. Similar to all Doppler technologies, assessment of myocardial strain by color-coded tissue Doppler requires an optimal Doppler angle, whereas the 2D speckle-tracking technique is less angle dependent. Despite the promise of these techniques, further research is required to determine their role in patients with repaired TOF.

Assessment of RV diastolic function by Doppler is susceptible to varying loading conditions and age. Consequently, standard Doppler indices of TV inflow are not reliable for assessment of RV diastolic function. Instead, a combination of Doppler profile in the MPA (including late diastolic antegrade flow), right atrial (RA) dilatation, hepatic venous flow reversal, and changes in the caliber of the IVC with the respiratory cycle are used. The implications of diastolic dysfunction in patients with repaired TOF are not entirely clear. Some authors have suggested that restrictive physiology in the right ventricle predicts superior exercise performance,[76] but this finding has not been confirmed by others.[77,78] The ASE guidelines recommend that the transtricuspid flow velocities be measured in the apical four-chamber window with the sample volume at the tips of the TV leaflets measured at end-expiration or averaging more than five consecutive beats. A tricuspid E/A ratio < 0.8 suggests impaired relaxation, and a tricuspid E/A ratio > 2.1 with a deceleration time < 120 msec suggests restrictive filling (particularly when accompanied by late diastolic forward flow into the MPA). As noted above, however, similar threshold values have not been ascertained in patients with repaired TOF.
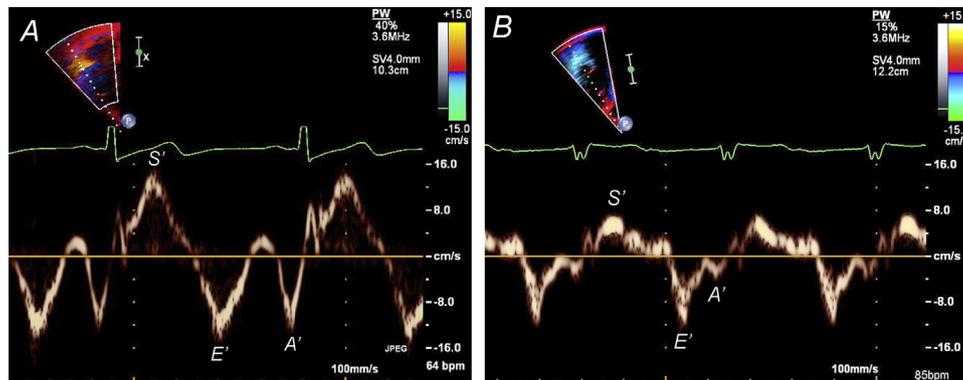
Figure 6 Tissue Doppler of **(A)** normal (peak S′ velocity, 14 cm/sec) and **(B)** depressed (peak S′ velocity, 7 cm/sec) RV systolic function.

iii. Pressure.–In adult patients, RA pressure is estimated by RA size and the respiratory variation in the size of the IVC. RA pressure is assumed to be 3 mm Hg when the IVC diameter measures ≤ 2.1 cm with >50% collapse, whereas with an IVC > 2.1 cm and <50% collapse, a high RA pressure of 15 mm Hg is assumed. An intermediate value of 8 mm Hg is used when IVC size and respiratory change do not fit the above scheme.[23] Similarly validated data are not available in infants and children.

Once the RA pressure has been established, RV or systolic PA pressure (in the absence of a residual RVOT obstruction) can be estimated using the TR jet velocity on the basis of the modified Bernoulli equation: $4v^2 +$ RA pressure. Using the modified Bernoulli equation, the mean and diastolic PA pressures can be estimated from the peak early and late diastolic velocities of the PR jet.[23] In many patients with repaired TOF, however, the pressure in the MPA and RV equilibrates in early or mid-diastole because of partial or complete absence of the PV. When the TR jet velocity indicates RV hypertension without an associated RVOT obstruction or identifiable branch PA stenosis, investigation for peripheral PA stenosis, pulmonary vascular disease, pulmonary vein stenosis, or left heart disease (e.g., cor triatriatum, mitral stenosis, diastolic LV dysfunction) should be carried out.

Right Atrium. RA measurements by 2D echocardiography are obtained as described by Rudski *et al.*[23] Measurements are performed at end-systole from the apical four-chamber view with the major axis obtained from the middle of the bisected TV annulus to the posterior wall of the right atrium and the minor axis taken at 90° to the major axis. In adult patients, RA area > 18 cm² indicates RA enlargement (Table 3). Normal values in children are not available.

In a study that compared RA size and function between 50 patients with repaired TOF and 30 normal controls, Hui *et al.*[79] found that RA size was increased (mean apical four-chamber area, 16.8 ± 5.5 vs 13.7 ± 5.1 cm²; *P* = .013) and emptying function was decreased (mean active emptying area fraction, 19 ± 9.8% vs 26.3 ± 10.3%, *P* = .005) after TOF repair. Similarly, RA systolic and diastolic strain values were lower in patients with TOF compared with controls.

LV Size and Function. Given that LV systolic dysfunction measured by EF has been shown to be an important prognostic marker for premature death in patients with repaired TOF,[50,80,81] its assessment is an essential element of the echocardiographic examination in this population. The size, global function, and regional wall motion of the left ventricle are determined from multiple views. Systolic flattening of the ventricular septum suggests

RV pressure overload, whereas diastolic septal flattening indicates volume overload. Measurement of LV systolic function by shortening fraction assumes a circular geometry with homogenous contraction, conditions that are seldom met in patients with repaired TOF. The biplane area-length method may be less susceptible to these assumptions and is preferred when technically feasible.[82] Measurements of LV volumes and EF by 3D echocardiography are preferred over 2D measurements. In patients with marked RV dilatation, the right ventricle is often apex forming, necessitating adjustment of the transducer position in the apical windows to avoid foreshortening of the left ventricle. In a study of 413 adult patients with repaired TOF, Diller *et al.*[83] recently showed that nongeometric indices of longitudinal LV function are associated with adverse clinical outcomes. Specifically, decreased mitral annular plane excursion measured from the apical window (analogous to TAPSE) and LV longitudinal strain were associated with the outcome independent of QRS duration.

Given that most patients with repaired TOF reach adulthood and the average age of this population continues to increase, the risk for development of acquired ischemic heart disease is likely to increase. Therefore, stress echocardiography may play an increasing role in this population.[84,85] Stress can be induced with exercise or through a pharmacologic agent (e.g., dobutamine).

Residual Shunts. The integrity of the VSD patch is determined by imaging and color Doppler flow mapping. Residual VSDs can be located at any part of the ventricular septum but are particularly common at the superior portion of the patch. These can usually be visualized by color Doppler from multiple imaging planes. Although a high-velocity systolic jet suggests that RV pressure is low, it should not be used independently to measure RV pressure, as the size of the VSD may vary during the cardiac cycle, and the jet may be eccentric. Similarly, the atrial septum is examined by color Doppler for the presence of a patent foramen ovale or a secundum atrial septal defect. Rarely, unrepaired sinus venosus defect, coronary sinus septal defect, or partially anomalous pulmonary venous connections are detected late after TOF repair.

Aortic Valve, Root, and Ascending Aorta. Dilatation of the aortic root is common in adults with repaired TOF, particularly those with prior shunts and those with late repair.[86,87] Measurements of the aortic root is accomplished from the parasternal long-axis view. Imaging from the right parasternal window can facilitate depiction and measurements of the proximal and mid ascending aorta. Measurements are made using 2D imaging according to published

guidelines in CHD during maximal expansion (mid to late systole).[88] Measurement of internal diameter is the current standard.[88,89]

Other Cardiovascular Issues. Confirmation of aortic arch sidedness is accomplished by imaging from the suprasternal short-axis aortic arch plane using both anterior and posterior tilt of the transducer to display the ascending and descending aorta. When the aortic arch is right-sided (as it is in about 25% of patients with TOF), the descending aorta may be seen coursing to the right. Additionally, identification of the innominate artery and its bifurcation into the left subclavian and left common carotid arteries is possible from the suprasternal window.

Evaluation of the origin and proximal course of the left and right coronary arteries can be clinically relevant in patients with repaired TOF. Although in many patients, this information is known before or during reparative surgery, previously undetected abnormal coronary anatomy can complicate reoperation or catheter intervention. The major challenge in echocardiographic delineation of coronary anatomy late after TOF repair relates to suboptimal acoustic windows.

d. Standard Protocol

Patient Preparation. Review of the patient's medical and surgical history, current medical condition, the specific questions for the echocardiographic study, and the patient's ability to cooperate with the examination should be ascertained before the scan commences. The patient's weight and height must be measured and recorded along with calculation of the BSA using an appropriate formula, such as the Haycock formula.[90] It is worth noting that the formula of DuBois and DuBois[91] does not cover the ranges of ages and body sizes encountered in patients with CHD and should not be used. Documentation of the body mass index may also be helpful. Additional steps taken before imaging begins include placement of electrocardiographic leads that avoid the standard echocardiographic imaging sites and recording the blood pressure and the heart rate. When pertinent, the blood pressure should be recorded on the opposite side of a previous Blalock-Taussig shunt.

Scanning Protocol. The ASE guidelines published in 2006 detail scanning protocols for the performance of pediatric echocardiography in patients with CHD,[92] and guidelines published in 2010 specify measurement techniques.[88] Importantly, each laboratory should follow a consistent detailed protocol that addresses the pertinent clinical issues in patients with repaired TOF. A sample echocardiographic protocol for patients with repaired TOF is listed in Table 2, and reference values for selected measurements are shown in Table 3.

e. Reporting Elements and Measurements

- RVOT and MPA
  - Dimensions
  - Location and mechanism of obstruction by 2D, color, and spectral Doppler
  - Presence of an aneurysm
  - Peak and mean gradients
- RV-to-PA conduit: peak and mean gradients
- Degree of PR on the basis of (1) regurgitation jet width by color Doppler, (2) spectral Doppler noting the duration and the slope (or pressure half-time) of the regurgitation jet, (3) presence and degree of flow reversal in the branch PAs, and (4) RPA pulsatility (systolic-diastolic diameter ratio)[93]
- Branch PAs
  - Dimensions of the narrowest and maximal segments
  - Location and severity of obstruction by 2D, color, and spectral Doppler

- Degree and mechanism of TR; if more than mild, measure (1) vena contracta width and (2) tethering height and area (optional)
- RV pressure on the basis of (1) TR jet velocity, (2) trans-VSD gradient, (3) systolic septal configuration (note the presence of right bundle branch block or septal dyskinesis)
- RV size and volume load on the basis of (1) TV annular diameter, (2) diastolic septal flattening, and (3) measurements of RV size as detailed above
- RV function on the basis of the parameters detailed above
- Residual VSDs: location, size, direction of flow, and peak transseptal gradient
- Residual atrial septal defects: location, size, and direction of flow
- Aortic dimensions: annulus, root, and ascending aorta at the level of the RPA
- AR
- Systemic-to-pulmonary collateral vessels on the basis of color Doppler interrogation and spectral Doppler evaluation of the abdominal aorta for diastolic runoff
- LV size and function

f. Transesophageal and Intracardiac Echocardiography

The primary role of TEE in patients with repaired TOF is for intraoperative assessment in conjunction with late interventions such as PV replacement and TV repair. Pre–cardiopulmonary bypass TEE may be performed to evaluate the atrial septum for the presence of a patent foramen ovale and the TV for the degree and mechanism of TR. TEE may be especially instrumental in the evaluation of the TV and PV as well as RV-to-PA conduits or the implanted PV for the presence of vegetations that were not detected by transthoracic imaging. After cardiopulmonary bypass, TEE is used to evaluate the repair and for functional assessment of the ventricles and valves. TEE or intracardiac echocardiography may also be used for guidance of transcatheter PV implantation[94] and device closure of residual atrial septal defects.

g. Recommendations

The committee recommends comprehensive echocardiographic evaluation for longitudinal follow-up of patients with repaired TOF through the use of a standardized examination protocol. Given that the management of chronic PR is a subject of intense research with ongoing evolution of therapies such as transcatheter PV implantation, the echocardiographic imaging protocol should be updated periodically as new information emerges. Integration of echocardiographic data with information from other modalities is imperative for optimal management of these patients, particularly given limitations of acoustic windows and assumptions of RV geometry that may well fail.

6. CARDIOVASCULAR MAGNETIC RESONANCE IMAGING

a. Overview of Modality

CMR is considered the reference standard for the quantification of RV size, RV function, and PR in patients with repaired TOF.[10] Through the use of multiple CMR techniques, different morphologic and hemodynamic aspects of the relevant pathophysiology are evaluated. In the context of this discussion, the most widely used imaging sequence is steady-state free precession (SSFP), which is a type of gradient-echo technique characterized by high signal-to-noise ratio, high T2/T1 contrast ratio, and sharp borders between the blood pool and the myocardium.[95] Electrocardiographically gated SSFP can be used as a cine magnetic resonance sequence, which is typically used for assessment of ventricular size and function, valve function, and intracardiac and extracardiac anatomy. Alternatively, an

Table 2 Example of an echocardiographic examination protocol in patients with repaired TOF

Imaging plane	Technique	Parameters	Goals and comments
Subxiphoid long-axis	• Supine • Knees bent • May require breath hold with inspiration	• LV length for 5/6 area × length (bullet) measurement • RV free wall thickness	• Visceral situs and cardiac position • Diaphragm function • RV/LV size and function • Atrial septum • Ventricular septum for residual VSDs
Subxiphoid short-axis	• Supine • Knees bent • May require breath hold with inspiration	• Doppler abdominal Ao for diastolic runoff • IVC: respiratory variation and diameter • Doppler hepatic veins • LV short-axis at papillary muscle level for 5/6 area × length measurement • Color and spectral Doppler in RVOT	• IVC diameter and collapse for RA pressure • Residual ASDs • Residual VSDs • RVOT obstruction • Mechanism of TR • Diastolic runoff in the abdominal Ao indicative of AR, systemic-to-pulmonary collateral vessels, or presence of a shunt
Subxiphoid "RAO" (counterclockwise 45° rotation from long-axis view allowing simultaneous visualization of RV inflow and outflow at the same time)	• Supine • Knees bent • May require breath hold with inspiration	• Color flow mapping and Doppler of the RVOT • 2D measurement of PV annulus and RPA	• Residual VSD (via patch leak or intramural egress) • Degree and location of RVOT obstruction • Doppler assessment of PR
Apical four-chamber	• Left lateral decubitus	• RA area (at end-systole) • TV annular lateral diameter • RV internal diameter at the base and mid levels at end-diastole • M-mode/2D of TV annulus for TAPSE • Modified Apical four-chamber optimizing RV for FAC • Color Doppler flow mapping of TR and measure vena contracta • Doppler TR for RV pressure • 3D when obtainable • AR by color and spectral Doppler • LV systolic and diastolic functional assessment (2D, Doppler) • DTI: lateral TV and MV annulus* • 2D strain	• RV optimization may be achieved by moving the transducer medially or laterally using the left ventricle as the window • Contemporaneous BP measurement preferred for TR gradient assessment opposite the site of the BT shunt (if pertinent) • Aim for high frame rates for DTI and 2D strain • Assess for regional wall motion abnormalities
Apical LV two-chamber	• Left lateral decubitus	• 2D measurements for LV volume	• Assess for regional wall motion abnormalities • Assess longitudinal strain
Apical three-chamber	• Left lateral decubitus	• AR by color and spectral Doppler	• Residual VSDs, especially subaortic
Parasternal long-axis	• Left lateral decubitus	• 2D measurement of TV AP diameter • Color and spectral Doppler of TR; measure vena contracta • Proximal and distal RVOT diameters • PV annulus and MPA • RVOT and MPA color and spectral Doppler • Aortic annulus and root dimensions • AR: location and measure vena contracta width	• Residual VSD • Degree of PR, TR, and AR • RVOT size and regional wall motion abnormalities • Aortic root and ascending Ao size

(Continued)

Table 2 (*Continued*)

Imaging plane	Technique	Parameters	Goals and comments
Parasternal short-axis	• Left lateral decubitus	• 2D measurement of proximal, distal RVOT, branch PAs • Color and spectral Doppler of RVOT, MPA and branch PAs • Color Doppler of AR jet	• PR: (1) jet width, (2) level and degree of diastolic flow reversal in the MPA and branch PAs, and (3) Doppler flow profile (deceleration rate) • RV size and function • LV size and function
Suprasternal notch (Ao short-axis)	• Supine • Extend the neck with slight head tilt to the left	• Arch sidedness and branching order • Presence and location of the left innominate vein • Rule out persistent LSVC and/or presence of anomalous pulmonary vein • 2D measurements of central and distal RPA • Color Doppler for BT shunt (if present)	• Follow the first vessel off the aortic arch for arch sidedness and for bifurcation indicative of normal vs mirror-image branching
Suprasternal notch (Ao arch long-axis)	• Supine • Extend the neck with slight head tilt to the left	• 2D measurement of LPA dimension • Color Doppler of the arch, assessing for diastolic flow reversal • Color Doppler for aortopulmonary collateral vessels • Rule out PDA	• Assess degree of aortic arch dilation • Pulse Doppler around the arch for degree of diastolic runoff to aid in determination of AR grade
Right parasternal (parasagittal)	• Right lateral decubitus • May require breath holding in expiration	• 2D measurement of ascending Ao • Color Doppler for residual ASD	• Dilated ascending aorta • Residual ASD

Ao, Aorta; *ASD*, atrial septal defect; *BT*, Blalock-Taussig; *BP*, blood pressure; *DTI*, Doppler tissue imaging; *FAC*, fractional area change; *LSVC*, left superior vena cava; *MV*, mitral valve; *PDA*, patent ductus arteriosus; *RAO*, right anterior oblique.
*Assessment of septal velocities is hampered by presence of the VSD patch.

electrocardiographically gated, respiratory-navigated SSFP sequence can yield a high–spatial resolution static 3D data set, which is often used for detailed assessment of intracardiac anatomy and/or coronary artery anatomy. Electrocardiographically gated turbo (fast) spin-echo (TSE) imaging offers high spatial resolution (submillimeter in-plane), excellent contrast between elements of soft tissue, and decreased sensitivity to metallic artifacts compared with gradient-echo sequences, although it provides only static images.

Contrast-enhanced magnetic resonance angiography (MRA) represents a robust 3D technique ideally suited for assessment of the arterial tree and the systemic and pulmonary veins. The acquisition of a 3D data set allows offline rendering of images in any arbitrary plane to best depict the anatomy in question, typically using a maximum intensity projection reconstruction technique. Alternatively, the anatomy can be displayed using surface or volume rendering techniques, which yield 3D models of cardiovascular structures. It should be noted, however, that contrast-enhanced 3D MRA is not synchronized with the cardiac cycle and is therefore subject to artifacts from cardiac motion. As a result, intracardiac morphology is affected by motion-induced blurring, although the great vessels are less affected and are typically seen well with this technique. Electrocardiographically gated, phase-contrast (PC) flow measurements are used for measurements of blood flow, including flow rates in the great arteries and veins, differential PA flow, and regurgitant volumes (e.g., PR, AR).

Several techniques are available for assessment of myocardial perfusion, ischemia, and scar tissue. The most commonly used technique for assessment of gross myocardial fibrosis in patients with repaired TOF is the late gadolinium enhancement (LGE) sequence. This technique has been shown to be helpful in this group of patients for identifying those at risk for ventricular tachyarrhythmias and exercise intolerance.[96,97]

The role of CMR in patients with repaired TOF varies according to age and clinical circumstance. During the first decade of life, the modality is used only when echocardiographic, electrocardiographic, and clinical data are either inconsistent or concerning for deterioration necessitating surgery or catheter intervention. Depending on the specific question, CMR may provide the necessary information to determine the best course of therapy. CMR is not recommended routinely in this age group, because the prevalence of major complications is low and echocardiographic windows are usually sufficient for adequate diagnostic evaluation. Once patients reach adolescence, however, CMR is recommended as a routine test for follow-up of RV size and function and PR. The rationale for that is that at this age group, the likelihood of adverse clinical outcomes increases, and echocardiographic windows often become more restricted. In addition, CMR does not require sedation in adolescents and adults. The ability of this modality to provide accurate quantitative information on biventricular size and function, blood flow measurements, myocardial viability, and cardiovascular anatomy has led to CMR's

Table 3 Echocardiographic reference values of RA and ventricular size and function in healthy adults (adapted from Rudski et al.[23])

Parameter	Abnormal
RV diameter (mm)	
Base	>42
Midventricular level	>35
RV diastolic length (mm)	>86
RV diaphragmatic wall thickness (subcostal view) (mm)	>5
Systolic function	
TAPSE (mm)	<16
Pulsed Doppler peak S′ (cm/sec)	<10
FAC (%)	<35
Diastolic function	
E/E′ ratio	>6
RA end-systolic area (cm^2)	>18
RA length (base to apex) (mm)	>53
RA lateral diameter (mm)	>44

FAC, Fractional area change.

becoming the preferred method of noninvasive imaging in adult patients with repaired TOF at many centers.[50,51,98-101]

b. Strengths and Limitations

CMR is ideally suited for assessment of repaired TOF because it allows comprehensive assessment of cardiovascular morphology and physiology without most of the limitations that hinder alternative imaging modalities. Specifically, CMR is independent of acoustic windows. It provides excellent image quality in patients with a wide range of body sizes and is not adversely affected by most surgical and catheter-based interventions. Another advantage of CMR is the absence of harmful ionizing radiation, making it appealing for longitudinal follow-up.[11] A notable strength of the modality is its ability to provide accurate and reproducible measurements of RV size and function, valve regurgitation, pulmonary and systemic flows, and differential PA flow and to detect scar tissue in the ventricular myocardium.

Limitations of CMR include a higher cost in comparison with echocardiography (but not in comparison with other modalities),[9] lack of portability, limited availability, artifacts from implants containing stainless steel,[102] and relative contraindication in patients with pacemakers or implantable defibrillators.[103] It is worth noting that certain old implants, such as stainless-steel coils and other devices with high metallic content, have been largely replaced by implants made of minimally or nonferromagnetic materials. More recently, the risk for nephrogenic systemic fibrosis that has been linked to gadolinium-based contrast has been mitigated by avoiding its use in patients with reduced glomerular filtration rates.[104] Importantly, when it comes to evaluation of the right heart by CMR, the use of a contrast agent is not a requirement.

c. Assessment of Repaired TOF with CMR

RVOT. Several imaging techniques, including cine SSFP, TSE, and contrast MRA, can be used to evaluate the RVOT. Cine imaging is advantageous because it depicts RVOT wall motion, allowing determination of akinetic or dyskinetic wall segments. This can be done in
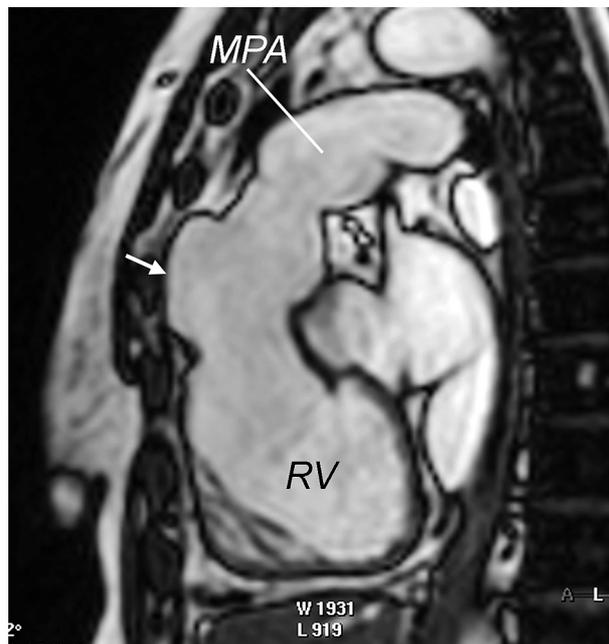
Figure 7 CMR SSFP image of an aneurysm of the RVOT (*arrow*).

a plane oriented to show the RV inflow and outflow, an axial plane, and an oblique sagittal plane through the long axis of the RVOT and MPA (Figure 7). Significant obstruction to flow across the RVOT is seen by a combination of observing anatomic narrowing on cine imaging and the presence of systolic signal flow void in that location. The SSFP sequence is also capable of detecting the presence of thrombus associated with an aneurysm of the RVOT, as illustrated in Figure 8. A volume-rendered MRA reconstruction allows a 3D representation of the outflow tract, including any aneurysm that may be present (Figure 9). CMR is helpful in understanding the RVOT geometry, which is an important element of planning percutaneous PV implantation.[105,106]

PAs. Branch PA anatomy is well visualized with CMR, and assessment of differential PA flow is measured with cine PC prescribed perpendicular to the vessels.[107] MRA is particularly valuable for imaging the PAs, as the 3D data set provides enhanced depth perception and visualization of complex anatomic relationships with neighboring structures (Figure 10). This modality has proved accurate in the evaluation of branch PA stenosis, with good agreement with traditional x-ray angiography.[108] Recently, the utility of MRA for planning interventions for PA stenosis has been reported.[109]

Imaging using TSE sequences is useful for depicting the extent and location of branch PA stenosis because of its higher spatial resolution. TSE sequences are also less susceptible to metallic artifacts and are used in patients in whom prior PA stents have been placed. However, their accuracy in depicting in-stent stenosis is not known. Nordmeyer *et al.*[110] demonstrated in an experimental model that gradient-echo, SSFP, and contrast CMR sequences are capable of assessing for in-stent stenosis.

PR. PR quantification is an important aspect of evaluation after TOF repair. Electrocardiographically gated free-breathing cine PC is the reference standard technique for flow measurements (Figure 11); in the case of PR measurement, this is performed perpendicular to the long-axis plane of the proximal MPA. PR fraction is calculated as retrograde flow volume divided by antegrade flow volume. In addition to
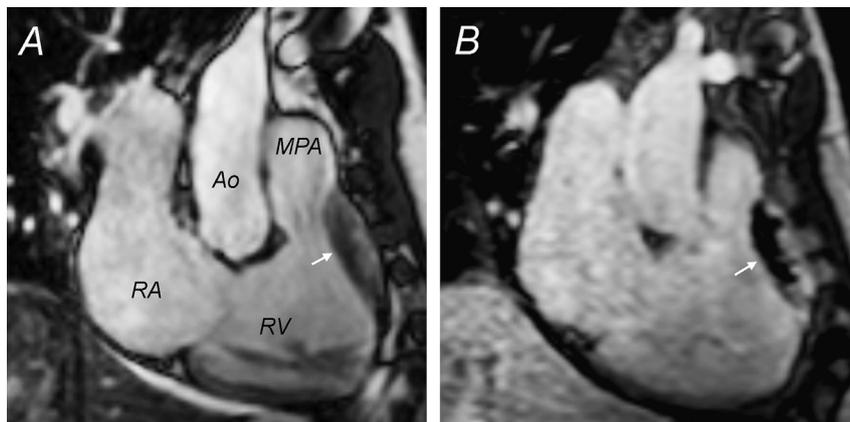
Figure 8 CMR evaluation of an RVOT aneurysm with thrombus (*arrow*) in a patient with repaired TOF. **(A)** SSFP. **(B)** LGE image with long inversion time in the same imaging plane showing no enhancement of the mass consistent with a thrombus. *Ao*, Aorta; *RA*, right atrium.
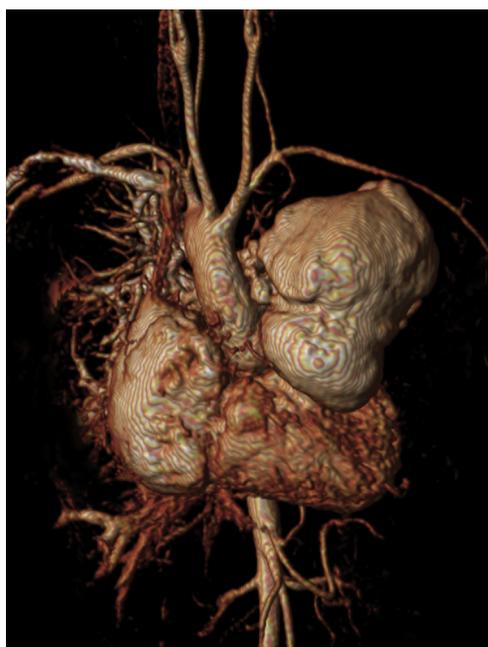
Figure 9 Volume-rendered gadolinium magnetic resonance angiographic reconstruction 3D representation of a large RVOT aneurysm.

Figure 10 Volume-rendered magnetic resonance angiographic reconstruction 3D representation of proximal branch RPA stenosis (*arrow*).

the PR fraction, the absolute value of the retrograde flow volume should be reported.[111] In the absence of a residual shunt, the net flow in the MPA and ascending aorta should be nearly identical. Similarly, in the absence of other valve regurgitation, shunt, or significant late diastolic antegrade flow in the MPA, LV and RV stroke volume differential is primarily affected by PR, and calculation of PR fraction by the two methods should be similar. In 15% to 20% of patients with repaired TOF, however, residual shunts and TR and/or AR are present, thus limiting the use of these comparisons.[112]

TV Morphology and Function. TV dysfunction is not rare in patients with repaired TOF, leading to TR that contributes to right heart dilatation. Mild or less TR is seen in most patients, whereas the frequency of at least moderate TR has been reported in 10% to 15% of patients.[39,112] The mechanisms of TR in this patient population

are discussed in the section on echocardiography. Although TEE remains the gold standard for detailed visualization of the atrioventricular valves, TV anatomy is well visualized in a stack of axial and short-axis cine SSFP acquisitions. In addition, an extended two-chamber RV view further depicts the TV in a vertical long-axis plane. The magnitude of TR can be quantified with cine PC oriented perpendicular to the TV inflow acquired in a four-chamber view at the level of the leaflets' tips. Quantification of TR has yet to be vigorously validated, in part because of the lack of a robust standard of reference with which measurements can be compared. The substantial through-plane motion of the TV poses a challenge for accurately measuring TV inflow.[113] Incorporating RV volumetric results with cine PC data may have inherent error greater than that for semilunar valve regurgitation.[114]

Right Ventricle. *i. Size and Function.*–Electrocardiographically gated cine SSFP is the current gold standard for quantitative evaluation of LV and RV volumes and mass.[9,10] Accurate determination of ventricular volume requires clear depiction of the blood-
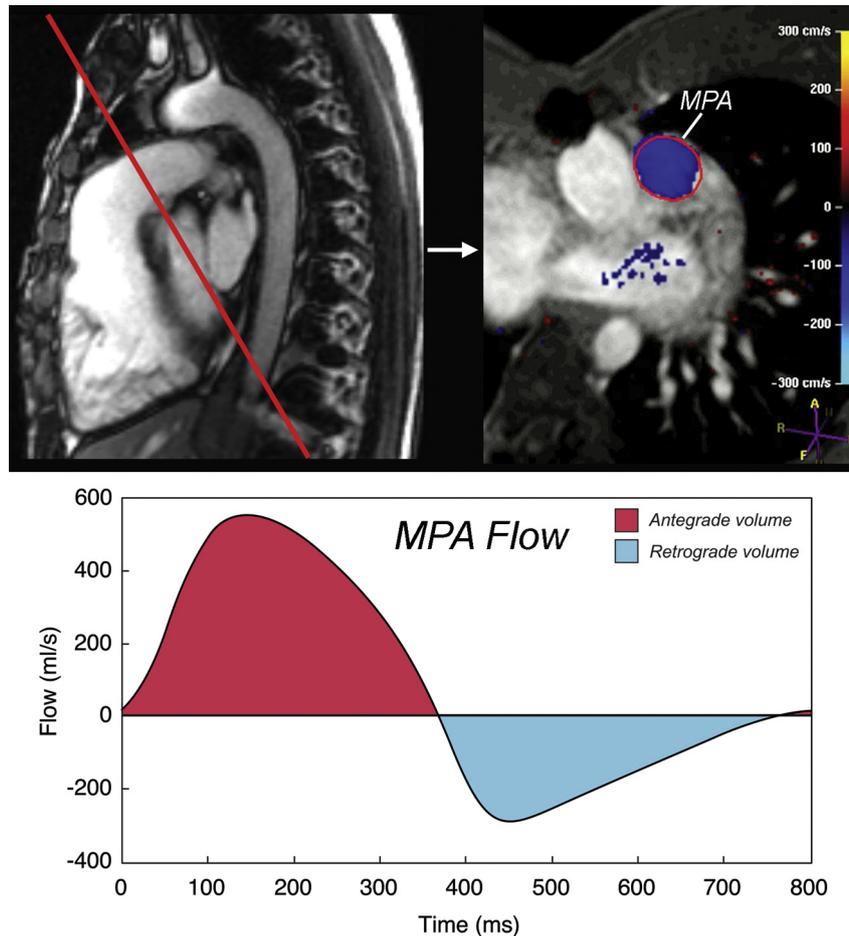
Figure 11 PA flow quantification in a patient with repaired TOF and severe PR. Imaging plane is positioned perpendicular to the proximal MPA (*top left*). Corresponding phase velocity map with region of interest drawn around the MPA flow signal (*top right*). Flow rate over time is shown in the lower panel. Volume and direction of flow is determined, and the PR fraction can be calculated by dividing the retrograde volume by the antegrade volume. This patient has severe PR with a regurgitation fraction of 44%.

myocardium boundary. Adjustments of the image brightness and contrast on the computer screen can facilitate visualization of that boundary. By tracing the blood-endocardium boundary, the slice's blood pool volume is calculated as the product of its cross-sectional area and thickness (which is prescribed by the operator). The LV papillary muscles and the major trabeculations of the right ventricle (e.g., septal band) are excluded from the blood pool and are considered part of the myocardium.[11,115] The ventricular volume is then determined by summation of the volumes of all slices. The process can be repeated for each frame in the cardiac cycle to obtain a continuous time-volume loop or may be performed only on end-diastolic (maximal area) and end-systolic (minimal area) frames to calculate diastolic and systolic volumes. From these data one can calculate ventricular stroke volumes and EFs. Because the patient's heart rate at the time of image acquisition is known, ventricular outputs can be calculated. Cross-referencing the short-axis images with LV and RV two-chamber (vertical long-axis) and four-chamber (horizontal long-axis) cine SSFP facilitates accurate determination of the atrioventricular and semilunar valves planes during systole and diastole.[116] In patients with repaired TOF, particular attention should be paid to determining the end-diastolic and end-systolic phases of each ventricle. Given that conduction delay is nearly universal in this population, peak RV contraction typically lags after that of the LV by one to three cardiac phases.[11]

Ventricular mass is calculated by tracing the epicardial borders and calculating the epicardial volume, subtracting the endocardial volume, and multiplying the resultant muscle volume by the specific gravity of the myocardium (1.05 g/mm^3). In the right ventricle, this measurement is challenging because of its trabecular morphology. One approach is to ignore the fine trabeculations and to trace the compacted free wall myocardium (the major septal trabeculations—septal and moderator bands—are excluded from the blood pool and considered RV mass).[115] Recent data indicates that this measurement is more reproducible when performed during systole compared with measurement in diastole.[117] An alternative approach is to use a semiautomatic threshold-based technique as described by Sarikouch *et al.*[118] The different approaches to contouring the myocardial trabeculations highlight the variations in practice that currently exist. Further research and technical advances are needed to improve the accuracy and reproducibility of these measurements.

From a clinical perspective, recent evidence indicates that increased RV mass measured by CMR in patients with repaired TOF is associated with greater risk for adverse outcomes, including sustained arrhythmia and death.[119] To optimize interstudy reproducibility in patients followed longitudinally, contours should be compared side by side with those from previous studies. Saving the contour files along with previous studies facilitates this comparison.

On average, total manual analysis time is about 25 to 30 min and decreases with operator experience.[11]

ii. Viability.—Through extensive research since the late 1990s, the LGE technique has been shown to be highly sensitive and specific for the presence of myocardial fibrosis.[120] In this technique, nonviable myocardium appears bright, whereas viable myocardium appears dark on images obtained 10 to 20 min after the administration of gadolinium contrast. LGE is also present as a result of inflammation, in the region of patch material, and other abnormalities of the myocardium. Presence of LGE has been associated with adverse clinical outcomes in patients with ischemic heart disease, cardiomyopathies, myocardial storage disorders, and valvular heart disease.[120,121] In patients with repaired TOF, LGE occurs commonly in locations of prior surgery (RVOT, VSD patch), as shown in Figure 12. In addition, LGE can also be found in the anterior RV free wall extending beyond the region of the patch in the left ventricle, and in the interventricular septum.[96,97] LGE in the superior and inferior junctions between the septum and the ventricular free wall is ubiquitous, and its clinical significance remains to be elucidated. A greater degree of LGE in these patients has been associated with exercise intolerance, ventricular dysfunction, and clinical arrhythmias.[96,97] However, it is unclear if LGE is associated with increased mortality in this patient population. The role of dobutamine stress CMR has been evaluated in small studies and awaits further study.[78,122,123]

Right Atrium. RA enlargement can be caused by significant TR and/or by increased RV end-diastolic pressure. A paucity of information is available on the range of RA dimensions and function in this population of patients. In a study comparing 20 patients with repaired TOF with seven healthy controls, Riesenkampff *et al.*[124] noted RA enlargement and abnormal reservoir and conduit function, which were associated with RV size and function. Specifically, patients with repaired TOF showed decreased early RA emptying, increased late emptying, and larger minimal RA volumes compared with controls. Patients with large RA and RV sizes showed the greatest degrees of LV diastolic function.[125] Further studies are required to shed light on the prognostic value of RA parameters with regard to clinical outcomes.

LV Size and Function. LV systolic dysfunction is present in up to 20% of adults with repaired TOF[126] and has been shown to be a strong independent predictor of death and sustained ventricular tachycardia.[50,80,81] A CMR investigation in 100 patients with repaired TOF demonstrated a close linear correlation between the EFs of the right and left ventricles.[50] This observation, which has been subsequently confirmed by other investigators, may be related to the "reverse Bernheim effect" relating RV dilatation and dysfunction, leading to LV dysfunction.[127] As discussed in the section on echocardiography, the precise mechanism or mechanisms that underlie adverse ventricular-ventricular interaction are a subject of current research.[128] Given the clinical importance of LV dysfunction in this group of patients, measurements of LV size, global and regional function, and viability are integral to the CMR examination protocol. Measurements of LV size and function are performed as described above for the right ventricle.

Residual Shunts. Although residual VSDs are usually diagnosed by color Doppler echocardiography, they can also be identified with SSFP or TSE imaging. Residual patch margin VSDs may be assessed by prescribing a stack of cine SSFP in plane parallel and perpendicular to the base of the ventricular septum, including the
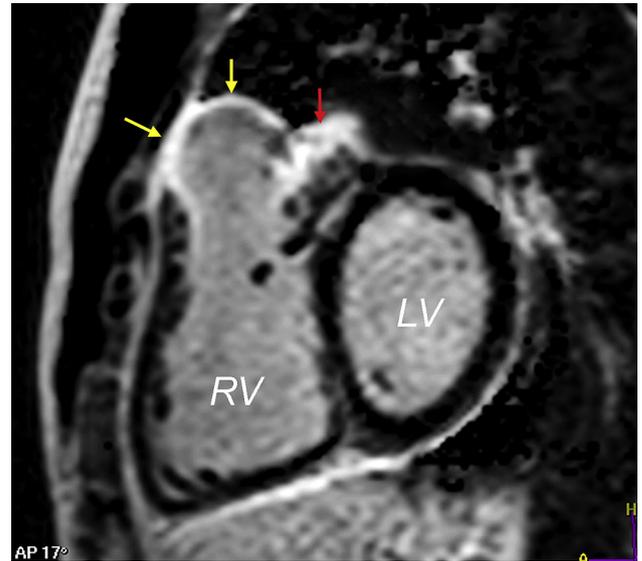
Figure 12 LGE image in ventricular short-axis showing late hyperenhancement (*yellow arrows*) of the RVOT patch. Note extension of the hyperenhancement to the superior wall of the right ventricle (RV; *red arrow*). *LV*, Left ventricle.

four-chamber plane, the three-chamber view highlighting the outflow tract, and the ventricular short axis. Similarly, the atrial septum is examined for a residual communication by cine SSFP, and MRA is used to exclude anomalous connections of the pulmonary veins. The magnitude of the systemic-to-pulmonary flow ratio can be accurately quantified by cine PC comparison of the net flow in the MPA and ascending aorta.[129]

Aortic Valve, Aortic Root, and Ascending Aorta. Close monitoring of the aortic root and ascending aorta for dilatation is routinely performed in patients with repaired TOF by obtaining cine SSFP sequences parallel and perpendicular to these locations. Electrocardiographically gated 3D SSFP is another technique that allows accurate and reproducible measurements of the proximal aorta without the use of a contrast medium.[130] Measurements of the great vessels are obtained from a cross-sectional image of the aorta (or PA) perpendicular to its long axis using a double-oblique approach as described by Kaiser *et al.*[131]

Contrast-enhanced MRA is also useful for evaluating and measuring the aortic root and ascending aorta. Ideally, the diameters of the aortic sinuses and sinotubular junction should be measured on electrocardiographically gated images to avoid motion artifacts and blurring. Consistent methods of acquisition and measurement are essential for the evaluation of any changes over time.[132] Aortic valve regurgitation fraction is measured by a cine PC sequence prescribed perpendicular to the aortic root.

Right aortic arch is found in approximately 25% of patients with TOF and is more common in those with chromosome 22q11 deletion. These patients are also more susceptible to abnormal branching patterns of the arch vessels. Rarely, repaired TOF can be associated with a previously undiagnosed vascular ring. The aortic arch and the brachiocephalic vessels are evaluated by MRA for arch sidedness and abnormal branching pattern.

Other Cardiovascular Issues. CMR is useful in evaluating the spatial relationships between cardiovascular structures and the airways. Another important role of CMR is to identify abnormal

coronary artery origins and proximal courses. This is particularly important in patients with prior repair who are being considered for percutaneous PV implantation.[133] The current adult CHD management guidelines recommend that coronary anatomy should be determined before any intervention on the RVOT (class I, level of evidence C).[12] Another consideration before reoperation in the patient with repaired TOF (e.g., PV replacement) is RV anterior wall and/or ascending aorta adherent to the posterior sternal table because these structures are at risk for accidental injury during sternotomy.

Noncardiac Findings. As patients with repaired TOF survive to an older age, one can anticipate a higher potential for identifying extracardiac findings by CMR. In a study of 240 CMR examinations done in non-CHD patients, 27% of studies were found to have previously unrecognized incidental findings, including pleural effusions, atelectasis, and adenopathy, as well as five cases of newly diagnosed malignancy.[134]

d. Standard Protocol

Patient Preparation. The importance of careful attention to details of patient preparation and placement in the scanner cannot be overemphasized. Optimal placement of electrocardiographic leads is paramount to quality gating. A peripheral intravenous cannula for injection of gadolinium-based contrast is placed in the following circumstances (subject to practice variations):

- First CMR examination
- >3 years since last LGE evaluation
- Deterioration in clinical status
- Regional or global ventricular function has worsened

Placement of an intravenous cannula in young patients may be deferred in settings in which attempts at intravenous cannula insertion might result in loss of patient cooperation.[11]

Scanning Protocol. An example of a CMR examination protocol for repaired TOF patients is listed in Table 4, and reference normal values for measurements are provided in Table 5. The examination protocol is designed to accomplish the following objectives:

- Quantitative assessment of RV and LV volumes, mass, stroke volumes, and EFs
- Evaluation of regional wall motion abnormalities
- Imaging the anatomy of the RVOT, PAs, aorta, and aortopulmonary collateral vessels
- Quantification of PR, TR, cardiac output, and pulmonary-to-systemic flow ratio
- Assessment of myocardial viability, with particular attention to scar tissue in the ventricular myocardium aside from sites of previous surgery (e.g., VSD and RVOT patches)
- Relationship of cardiovascular structures to the sternum

e. Reporting Elements and Measurements

- RVOT obstruction and or aneurysm; length of dyskinetic segment
- Branch PA stenosis
- RV and LV size and function (absolute and BSA-adjusted values): end-diastolic volume, end-systolic volume, stroke volume, EF, mass, mass-to-volume ratio
- Vessel dimensions: aortic root, ascending aorta, MPA, RPA, LPA
- RA size by the area-length method[135]
- Flow measurements
  - ◦ Ascending aorta, MPA, RPA, LPA
  - ◦ PR fraction and volume
  - ◦ Other valve regurgitation
- LGE presence and extent

f. Recommendations

CMR is recommended in young patients (usually ≤10 years) when the echocardiographic and clinical data are concerning for unfavorable disease progression (e.g., ventricular dysfunction, right heart failure symptoms). Once patients reach adolescence, CMR is performed routinely using a comprehensive imaging protocol. Quantitative assessment of ventricular size and function and PR, for which CMR is the reference standard, are essential elements of the imaging protocol.

7. CARDIOVASCULAR COMPUTED TOMOGRAPHY

a. Overview of Modality

Widespread availability of CT has lead to increased utilization of this noninvasive modality in the general population.[136] Early challenges with motion artifacts encountered with imaging complex congenital anatomy throughout the cardiac cycle limited the evolution of this application in the assessment of this patient population. However, advances in multidetector computed tomographic technology have led to improvements in both spatial and temporal resolutions, allowing the acquisition of a volume of data during a single breath-hold examination.[137] Subsequently, the ability to produce static images of the heart and great vessels as well as 3D reconstructions has revolutionized this technique and propelled cardiac CT into the arena of anatomic imaging of patients with complex CHD.

In general with MDCT, the x-ray point source(s) and the detector array are located on opposite sides of the patient on a ringlike structure called a gantry. The gantry rotates around the patient, located at the table center. The table then moves at a constant speed as x-rays penetrate the patient and are captured by one or more of the detectors. Once complete, a series of helical projections are generated. From these data, images representing x-ray attenuation from each point in the volume are mathematically reconstructed.[138] Certain scanners are capable of volume scanning without table movement.[139]

Scanners with fewer detectors create an image set from data acquired from several heartbeats. To improve overall quality of computed tomographic images and ensure a longer diastolic window with minimal cardiac motion, pharmacologic heart rate control is frequently used. Successful prescan heart rate control facilitates postprocessing that requires image reconstruction of the data set in a fixed interval preceding the R wave. Furthermore, heart rate optimization avoids gating errors associated with heart rate changes that may occur during image acquisition and that lead to image artifacts. These strategies are particularly important in the evaluation of the coronary arteries and ascending aorta to avoid motion artifacts that occur throughout the cardiac cycle. Therefore, heart rate control with oral or intravenous β-blockade is advised before CT for patients without contraindications.[140]

Data postprocessing commences after image acquisition is complete. Postprocessing includes (1) electrocardiographic review for ectopic beats or arrhythmias, (2) selection of the optimal phase for reconstruction, (3) selection of appropriate reconstruction parameters and kernels, (4) review of the axial (source) data set, and (5)

Table 4 Example of a CMR examination protocol in patients with repaired TOF (adapted from Geva[11])

Sequence	Technique	Imaging planes	Parameters	Goals and comments
Localizing images	• ECG-gated SSFP • Real-time interactive SSFP	• Axial, coronal, and sagittal • Multiple oblique planes		Anatomic survey and planning subsequent sequences
Cine MR evaluation of anatomy and ventricular and valve function	• ECG triggered, breath-hold cine SSFP	• LV two-chamber (vertical long-axis) • RV two-chamber (vertical long-axis) • Four-chamber (horizontal long-axis) • RVOT long-axis • LVOT long-axis • Axial stack: RVOT and PAs	TE, 1.7 msec; TR, 3.3 msec; flip angle, 60°; SENSE acceleration factor, 2; FOV, 260 mm; matrix size, 160 × 160 reconstructed to 256 × 256; voxel size, 1.6 × 1.8 × 6–8 mm reconstructed to 1.0 × 1.0 × 6–8 mm; 30 reconstructed images per cardiac cycle	Evaluation of intracardiac anatomy, residual septal defects, outflow tract obstruction
Cine MR evaluation of ventricular volumes and mass	ECG triggered, breath-hold cine SSFP	Ventricular short-axis	Same parameters; 12–14 equidistant slices (slice thickness, 6–8 mm; interslice space, 0–2 mm) covering the entire length of both ventricles	Attention to inclusion of the base of the right and left ventricles at end-diastole with addition of extra slices as needed for complete coverage
Gadolinium-enhanced 3D MR angiography	Non-ECG triggered 3D spoiled gradient-echo	Sagittal or coronal	TE, 1.5 msec; TR, 4.5 msec; flip angle, 40°; voxel size, 1.0 × 1.0 × 2.4 mm reconstructed to 0.7 × 0.7 × 1.2 mm; two acquisitions, each lasting ~20 sec	• Used for evaluation of vascular anatomy and RVOT morphology • Alternative approaches: (1) two high spatial resolution acquisitions, (2) time-resolved MRA
Flow measurements	ECG triggered, breathe-through cine PC	Perpendicular to the proximal MPA, ascending aorta, and AV valves (branch PAs optional)	TE, 3.7 msec; TR, 5.9 msec; flip angle, 15°; SENSE factor, 2; FOV, 300 mm; matrix size, 192 × 192; voxel size, 1.6 × 1.6 × 6.0 mm reconstructed to 1.2 × 1.2 × 6.0 mm; 40 reconstructed images per cardiac cycle	Quantification of PR, other valve regurgitation, pulmonary and systemic flow, differential PA flow
LGE	ECG triggered, breath-hold, phase-sensitive LGE	Ventricular short-axis, LV two-chamber, LV three-chamber, RV two-chamber, and four-chamber	TE, 3.5 msec; TR, 5.9 msec; flip angle, 20°; FOV, 260 mm; matrix size, 144 × 144; voxel size, 1.8 × 1.8 × 7–8 mm reconstructed to 1.0 × 1.0 × 7–8 mm	Identification of myocardial scar tissue

AV, Atrioventricular; *ECG*, electrocardiographically; *FOV*, field of view; *LVOT*, LV outflow tract; *MR*, magnetic resonance; *SENSE*, sensitivity encoding; *TE*, echo time; *TR*, repetition time.
Additional case-specific sequences include (1) cine SSFP in the short axis of the aortic root and ascending aorta in patients with dilated aortic root and ascending aorta; (2) TSE sequence with blood suppression for imaging of the outflow tracts and branch PAs in patients with image artifacts from metallic implants; (3) ECG triggered, respiratory navigated, free-breathing 3D isotropic SSFP for evaluation of the coronary arteries or as a substitute for contrast MRA; and (4) T1 mapping for evaluation of diffuse myocardial fibrosis.

Table 5 Selected normal values of chamber size and function by CMR

Parameter	Study				
	Alfakih et al.[191]	Hudsmith et al.[192]	Sarikouch et al.[118]	Robbers-Visser et al.[194]	Buechel et al.[195]
Age (y)	43 (20–65)	38 (21–68)	11.9 (4–20)	8–17	11 (0.7–18)
Sample size	60	108	114	60	50
PMs excluded from blood pool	Yes	Yes	Yes	Yes	No
Ventricular volumes and function					
LV EDV (mL/m^2)					
Male	82.3 ± 14.7	82 ± 13	85.1 ± 13.8	79 ± 11	77.5 × BSA$^{1.38}$
Female	77.7 ± 10.8	78 ± 12	77.9 ± 10.8	71 ± 8	67.8 × BSA$^{1.38}$
LV EF (%)					
Male	64.2 ± 4.6	69 ± 6	64.4 ± 4.9	69 ± 5	61.3 ± 4.1
Female	64.0 ± 4.0	69 ± 6	63.4 ± 6.1	69 ± 5	
RV EDV (mL/m^2)					
Male	86.2 ± 14.1	96 ± 15	84.5 ±12.7	86 ± 12	83.8 × BSA$^{1.47}$
Female	75.2 ± 13.8	84 ± 17	76.9 ± 12.7	73 ± 9	72.7 × BSA$^{1.47}$
RV EF (%)					
Male	55.1 ± 3.7	59 ± 6	61.6 ± 4.5	65 ± 5	58.2 ± 3.6
Female	59.8 ± 5.0	63 ± 5	62.8 ± 4.3	65 ± 5	
Atrial volumes			Sarikouch et al.[193],*		
LA volume (mL/m^2)					
Male			46.7 ± 10.1		
Female			44.2 ± 8.7		
RA volume (mL/m^2)					
Male			58.1 ± 15.7		
Female			53.3 ± 11.8		

EDV, End-diastolic volume; *ESV*, end-systolic volume; *LA*, left atrial; *PM*, papillary muscle.
Data are expressed as mean (range) or as mean ± SD.
*Sample size n = 115; mean age, 12.4 years (range, 4.4–20.3 years).

evaluation of anatomic abnormalities using multiplanar reformats, including true short-axis as well as long-axis maximum intensity projection images.[141]

As a result of these advances in computed tomographic technology, MDCT is now emerging as a complementary modality to established noninvasive imaging techniques as well as a viable alternative in those with absolute contraindications to CMR.[142]

b. Strengths and Limitations

The major advantage of CT in patients with repaired TOF is its excellent (usually submillimeter) spatial resolution. With well-timed, high-quality computed tomographic angiography, the contrast-to-noise ratio is also excellent. Thus, electrocardiographically gated computed tomographic angiography provides a very clear depiction of cardiovascular anatomy. This advantage is particularly valuable for detailed evaluation of small blood vessels such as the coronary arteries or the distal PA branches. Another advantage is the ability to perform CT in patients with pacemakers and defibrillators. Additionally, CT may allow successful imaging of structures that are obscured on CMR imaging by stainless-steel metallic artifacts.

CT has several noteworthy limitations. As with any modality that uses ionizing radiation, exposure increases the risk for cancer.[143-145] This risk increases with a higher radiation dose, repeated exposures, younger age, and female gender.[146,147] Electrocardiographically gated cardiac CT is associated with a higher radiation dose compared with a nongated scan. Another limitation of cardiac CT is lower temporal resolution compared with echocardiography and CMR. In addition, compared with these modalities, CT does not provide hemodynamic information on flow rate or velocity. Finally, the use of contrast is associated with risk for renal dysfunction in patients with impaired renal function.[148]

c. Assessment of Repaired TOF with CT

PAs. The spectrum of morphologic abnormalities of the PAs, including obstruction, stenosis, aneurysmal dilatation, and abnormal course, can be evaluated with MDCT.[149,150] Abnormalities in PA architecture are often the result of prior palliative repairs and shunt-related complications. The PA architecture should be inspected in patients with repaired TOF and with particular scrutiny in those with prior palliative repair.

As the use of catheter-based interventions for treatment of branch PA stenosis or hypoplasia increases, about 22% of patients may develop further complications, including intimal hyperplasia, stent fracture, dissection, or aneurysm formation, requiring reintervention or close surveillance.[151] MDCT provides accurate assessment of the anatomy of the stented segments as well as surrounding anatomic structures (Figure 13). To improve visualization of the stented segment, selection of a "hard" kernel before reconstruction of the source image set may result in increased spatial resolution and edge detection. However, the cost for improved spatial resolution is greater image noise. In contrast to the routine evaluation of the coronary artery stent, the larger stents encountered in patients with repaired TOF do not obscure visualization of the lumen, nor do the stent struts cause significant beam-hardening artifacts. Therefore, "harder" reconstruction kernels to assess stent patency have not been routinely used in this population.
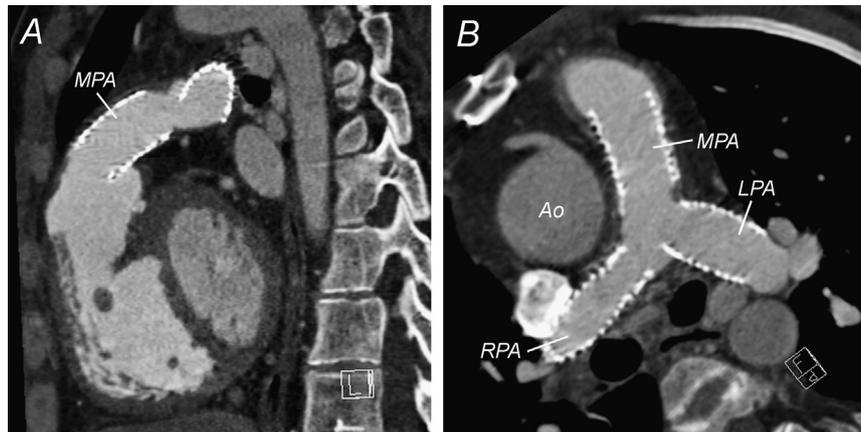
Figure 13 CT of the RVOT and PAs in the sagittal **(A)** and axial **(B)** planes showing unobstructed stents. *Ao*, Aorta.

RV and LV Size and Function. Biventricular volumes are assessed by retrospective reconstruction of the initial data set acquired during electrocardiographically gated MDCT at multiple phases of the cardiac cycle. The computed tomographic data volume is then reconstructed at 5% or 10% intervals from 5% to 95% of the R-R interval, providing a multiphase data set to obtain end-diastolic and end-systolic volumes of the left and right ventricles. From this, stroke volume, cardiac output, LV EF, and RV EF are calculated.[152] Dedicated semiautomated software is available to assist in the determination of ventricular volumes and function. However, because of the complex geometry of the right ventricle, these semiautomated techniques are often not reliable. CMR remains the gold standard in the assessment of RV function in adults with CHD, but MDCT accurately quantifies RV measurements and demonstrates close correlation to CMR.[153,154] Therefore, MDCT offers an alternative imaging strategy in patients with absolute contraindications to CMR.

Aortic Valve, Aortic Root, and Ascending Aorta. Utilization of cardiac CT has been well described in the assessment of diseases of the aorta.[155] In addition to other conotruncal anomalies, moderate dilatation of the ascending aorta is also encountered in adults with repaired TOF. Rarely, reports of dissection have occurred in adults with repaired TOF and massive aortic dilatation.[156,157] Although there are no established guidelines for serial evaluation of the ascending thoracic aorta to determine risk for progressive aortic root dilatation or dissection, these case reports highlight the need for meticulous follow-up and evaluation of the aortic root after repair of TOF.

Therefore, a comprehensive multidetector computed tomographic examination in patients with repaired TOF should include at the very least examination of the ascending thoracic aorta to obtain measurements of size. The scan protocol should include electrocardiographic gating to provide accurate measurements of the aorta and avoid misdiagnosis of aortic dissection secondary to motion artifact simulating an intimal flap. Measurements of the aorta with MDCT should include both luminal and wall thickness perpendicular to the axis of blood flow.[158] Mao *et al.*[159] evaluated thoracic aortic diameters in a large population of patients without known disease to establish normal values on the basis of age and gender. The interobserver, intraobserver, and repeated measurement correlations for measurements of the aorta (wall thickness and lumen) were high ($r > 0.91$, $P < .001$).

Other Cardiovascular Issues. *i. Coronary Arteries.*–The prognostic role of MDCT as well as its ability to characterize complex coronary artery anatomy has been thoroughly investigated.[160-162]

Although there have been several advances in the evaluation of coronary artery anatomy and atherosclerosis with CMR imaging, MDCT remains a favorable imaging technique with higher diagnostic performance and accuracy in the evaluation of coronary artery stenosis.[163] Still, in patients with repaired TOF, the goal of coronary artery imaging usually centers on the origins, proximal courses, and spatial relationships to neighboring structures.

Preoperative assessment with MDCT provides a noninvasive method to evaluate coronary artery anatomy before subsequent reoperation (Figure 14). This application provides a detailed assessment of the origin, course, and anatomy of the coronary arteries as well as the 3D relationship of the coronary arteries to the great vessels that is often helpful during the preoperative assessment of adults with CHD.[164] Although there are no established guidelines for such preoperative multidetector computed tomographic evaluation, this technique may identify concerning findings that can influence surgical planning (Figure 15).

Noncardiac Findings. MDCT can provide additional insight into abnormalities of the airways, lung parenchyma, pericardial and pleural spaces, and mediastinum. The modality is particularly sensitive to the presence of adenopathy, other thoracic masses, and abnormalities of the lung parenchyma such as emphysema.

d. Standard Protocol

Cardiac MDCT in patients with repaired TOF requires particular attention to detail in addition to a comprehensive review of medical and surgical history. Insufficient prescan planning and inaccurate contrast administration during MDCT can lead to inappropriate exposures to nephrotoxic contrast and ionizing radiation. To avoid potential errors at the time of cardiac MDCT, the protocol should not only be tailored to each case but also reviewed with the referring physician to ensure that the clinician's needs are addressed by the scan protocol.

Patient Preparation. Upon patient arrival, a review of study indication, prior medical and surgical records, and screening for contraindications should be performed. After placement of an 18-gauge or 20-gauge intravenous cannula, heart rate control should be initiated according to laboratory protocol. Oral β-blockers are often prescribed before the examination to ensure adequate heart rate control. If additional heart rate control is required at the time of examination, this can be achieved through intravenous administration of β-blockers or calcium channel blockers.
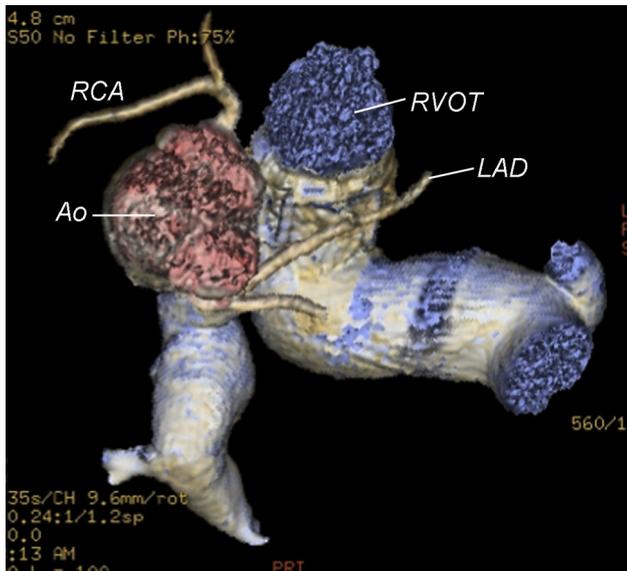
Figure 14 Computed tomographic 3D reconstruction demonstrating coronary artery anatomy in a patient with repaired TOF. *Ao*, Aorta; *LAD*, left anterior descending coronary artery; *RCA*, right coronary artery.

Scanning Protocol. The following is an example of cardiac MDCT using a 64-slice scanner: 0.6-mm collimation, tube voltage (80–120 kVp), and tube current–time product adjusted to body mass index with electrocardiographic dose modulation to minimize radiation exposure.[165] In most patients, the scan coverage is from the carina to the base of the heart (1 cm below the diaphragm). However, if there is any concern for abnormalities of the thoracic aorta, the anatomic coverage should be extended superiorly to adequately cover the brachiocephalic vessels. A dual-head power injector is used to inject contrast through a peripheral intravenous cannula during an inspiratory breath-hold (15–20 sec long) and retrospective electrocardiographic gating. The dose of contrast varies according to body size and scanning protocol. This is then followed by a saline flush (60 mL) at 4 mL/sec to facilitate contrast delivery and diminish beam-hardening contrast artifact in the superior vena cava. However, each cardiac multidetector computed tomographic protocol is tailored accordingly to the clinical questions asked at the time of examination.

If the clinical question is to evaluate branch PAs, after interventional therapy of the PAs, and/or RV size and function, the study should then be optimized to opacify the structures of interest. Therefore, a timing bolus optimized to the MPA at the level of the carina using 110 Hounsfield units for initiation of the scan will optimize contrast opacification of these structures.

Alternatively, if the clinical question is to evaluate LV size and systolic function, coronary artery anatomy, and/or aortic root anatomy, the study should be optimized to the left-sided structures. Here, the region of interest for the timing bolus should be located in the ascending aorta at the level of the carina using 110 Hounsfield units or initiation of the scan. Again, the scanning distance should be extended superiorly to the brachiocephalic vessels if there is concern for abnormalities of the aortic root.

To obtain anatomic information regarding both the left and right heart during a single cardiac multidetector computed tomographic examination, regions of interest should be placed in both the aorta and the MPA. The test bolus is then performed to determine the intersection of maximum Hounsfield units concentration in both great vessels to provide adequate opacification of both circulations. Using this type of a protocol, information regarding both PA and aortic architecture is available in addition to biventricular volumes and function.

Scan Reconstruction. To optimize 3D imaging, scans are then reconstructed with a slice thickness of 0.6 mm and a slice overlap of 0.6 mm. The postprocessing protocol for calculation of ventricular volumes and EFs includes reconstruction of multiphase short-axis images in 5% to 10% increments of the R-R interval (5%–95%).

e. Recommendations

We recommend that given the young age of this population, every effort should be directed toward radiation reduction strategies implemented during the time of examination. The most effective technique to reduce radiation dose in young adults with CHD is to avoid exposure. Therefore, CMR should remain the imaging modality of choice in patients with repaired TOF, and cardiac MDCT should be reserved for patients with absolute contraindications to CMR, particularly given the need for serial examinations.

8. NUCLEAR SCINTIGRAPHY

a. Overview of Modality

Nuclear cardiology is a physiologic diagnostic modality that uses radioisotope-labeled compounds to capture and quantify blood flow, myocardial perfusion and integrity, and ventricular function. Historically, radionuclide imaging has been used for the evaluation of ventricular function, pulmonary perfusion, and quantification of cardiac shunts in patients with CHD, including repaired TOF. However, many of these indications are now more readily evaluated with CMR, which provides superior anatomic delineation and does not require the radiation exposure inherent in radionuclide imaging. In patients who are unable to undergo CMR, nuclear scintigraphy is a reasonable alternative for quantification of differential PA blood flow. In highly selected circumstances, nuclear scintigraphy can be used for assessment of ventricular function and myocardial perfusion and viability in this population.

b. Strengths and Limitations

Nuclear scintigraphy is a robust technique for measuring differential pulmonary blood flow.[166] In the presence of multiple sources of blood supply to the lungs, however, this technique is not accurate. The role of this modality is well established in the evaluation of LV perfusion and viability.[167] However, several technical limitations hinder its application to the assessment of the RV myocardium. Compared with other noninvasive imaging modalities, nuclear scintigraphy is not considered a robust technique for assessment of RV size, function, regional wall motion abnormalities, or anatomic anomalies. Importantly, nuclear scintigraphy exposes patients to ionizing radiation with its attendant risk for cancer. Given that many patients with repaired TOF require multiple evaluations, the radiation risk increases with each exposure.

c. Assessment of Repaired TOF with Nuclear Angiography

PAs. Measurement of pulmonary perfusion is an important part of the evaluation in patients with repaired TOF and suspected branch PA stenosis. Up to 20% of these patients have been reported to develop significant branch PA stenosis.[168] Regional perfusion differences within
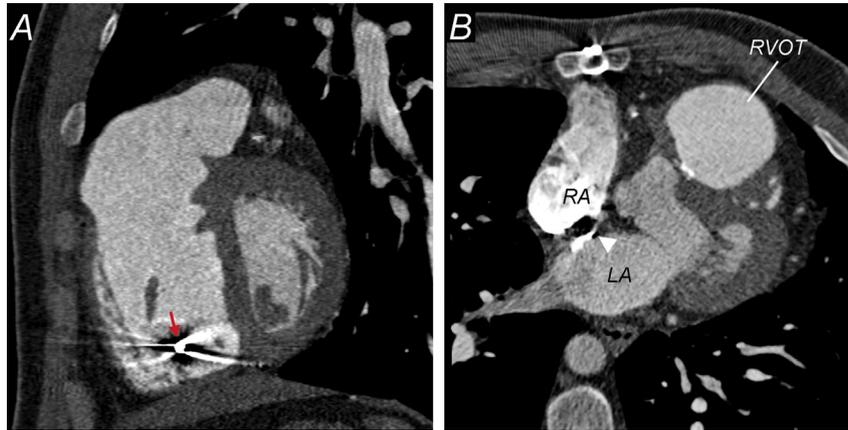
Figure 15 CT in a patient with repaired TOF and severe PR who is a candidate for PV replacement. **(A)** Note pacemaker lead in the right ventricle (*arrow*) and proximity of the RVOT to the sternum. **(B)** Note patent foramen ovale (*arrowhead*). *LA*, Left atrium; *RA*, right atrium.

the lungs are also common and may be a result of the presence of native branch stenosis, PA obstruction after a surgical shunt, segmental or lobar pulmonary vascular disease, or associated arborization anomalies with large aortopulmonary collateral vessels.[169] Lung perfusion scintigraphy uses ^{99m}Tc-labeled macroaggregates of albumin that embolize to the capillary level and provide an accurate picture of the differential lung perfusion ratio.[170,171] In patients with repaired TOF, measurements of differential pulmonary blood flow and regional lung perfusion have a well-established record before and after treatment of branch PA stenosis.[166,171-174]

Right Ventricle. i. Size and Function.–Radionuclide angiography can provide quantitative assessment of RV EF. It is a noninvasive test, and the results can be used to follow ventricular function over time.[175-177] This method of assessing RV function, however, provides limited morphologic information. It is used sparingly for this indication and almost exclusively in patients who have contraindications to CMR and cardiac CT.

ii. Viability.–There is very little role for myocardial perfusion scintigraphy in children with repaired TOF. However, a growing number of patients with repaired TOF reach older age and thus become more likely to develop coronary artery disease. Anecdotal reports on this subject have been published.[178] Therefore, evaluation of myocardial perfusion and viability in these patients by nuclear techniques is considered on a case-by-case basis.

Noncardiac Findings. In addition to the indications noted above, a ventilation scan can be performed in conjunction with a lung perfusion scan. This test allows quantitative assessment of ventilation-perfusion mismatch.

d. Standard Protocol

Standard protocols for performance of pulmonary perfusion scintigraphy, radionuclide ventriculography, and myocardial perfusion scintigraphy in children and adults are published and updated by the American College of Radiology, the Society for Pediatric Radiology, and the Society of Nuclear Medicine and Molecular Imaging and are displayed on their Web sites.[179,180]

e. Recommendations

We recommend the use of radionuclide scintigraphy for evaluation of differential pulmonary blood flow and regional lung perfusion when

the information cannot be obtained by CMR. The modality may also be used in highly selected cases when other modalities are not practical for assessment of ventricular volume and function and myocardial perfusion and viability.

9. X-RAY ANGIOGRAPHY

a. Overview of Modality

Diagnostic cardiac catheterization with x-ray angiography is rarely used primarily for diagnostic imaging purposes in patients with repaired TOF. However, it serves an important role when essential information cannot be accurately obtained noninvasively, particularly for those in whom echocardiographic data are inconclusive or contradictory and CMR is contraindicated. Additionally, x-ray angiography is an integral component of catheter-based procedures such as PA balloon dilation and stenting, percutaneous PV implantation, management of aortopulmonary collateral vessels, closure of residual septal defects, and coronary artery interventions.[133,181,182]

A complete right and left heart catheterization is performed before angiography and allows evaluation of the presence of residual shunt by oximetry, diastolic dysfunction by measurements of filling pressures, stenosis by pullback gradients, and PR by loss of the dicrotic notch in the PA tracings and equilibration of diastolic pressures between the MPA and right ventricle. In addition, cardiac index is estimated by oximetry or thermodilution, and pulmonary and systemic vascular resistances are calculated. In the presence of significant TR and/or PR and when a residual shunt is present, cardiac output is better calculated by oximetry using the Fick principle. In the presence of proximal branch PA stenosis, pulmonary vascular resistance can be calculated using the Fick principle and knowledge of differential PA blood flow from a lung perfusion scan or CMR.[183]

b. Strengths and Limitations

Diagnostic cardiac catheterization with x-ray angiography is considered the gold-standard modality for assessment of intracardiac pressures, coronary arteries beyond their origins, and branch PAs. Important limitations of the modality include its invasive nature and associated morbidity, high cost, and exposure to ionizing radiation. For these

Figure 16 Example of rotational angiography performed in the right ventricle (RV) after repair of TOF demonstrates severe bilateral branch PA stenosis. On the RPA (*asterisk*), a stent was implanted proximally, and there is severe stenosis at the distal end of the stent (*arrow*). Image courtesy of Dr Matthew Gillespie, Children's Hospital of Philadelphia.

reasons, the modality is used solely for diagnosis only in carefully selected cases. Given that the number of patients with repaired TOF reaching the age range when coronary artery disease is prevalent, the role of diagnostic imaging of the coronary arteries will likely increase.

c. Assessment of Repaired TOF with X-Ray Angiography

RVOT. In addition to biplane angiography, rotational angiography is a relatively new technology that is increasingly being used for assessment of patients with CHD. In patients with repaired TOF, this technique is particularly useful for visualizing proximal bifurcation PA stenosis and RVOT anatomy, especially in the presence of a conduit-associated branch PA stenosis (Figure 16).[184,185]

Rotational angiography is performed over 200° using a large-format, digital, flat-panel angiographic system. Images are acquired with low radiation doses using a slow injection of a small amount of contrast media. The acquisition can be performed under rapid ventricular pacing to slow the contrast washout and reduce motion artifacts. Three-dimensional angiographic images are generated on a workstation in near real time during the procedure. Different acquisition and display parameters can be used. For example, Glatz *et al.*[185] used 190° rotation, nongated 5-sec acquisition time, projection on either 20×20 cm or 30×40 cm flat-panel detector size, and 48-cm field of view. They displayed the tomographic volume set at a slice thickness of 0.3 mm, although this can be variable. Breath holding is used when possible, and radiation dose is adjusted to minimize exposure while maintaining adequate image quality. The intravenous contrast agent is diluted with 2 mL saline for each milliliter of contrast, for a total volume of approximately 1.5 mL/kg per injection. The reconstructed 3D image can then be projected as an overlay on the live fluoroscopy monitor, which facilitates complex catheter manipulations. It can also be useful for defining optimal camera angles for standard biplane angiography or fluoroscopic guidance. The main advantage is that it provides a more
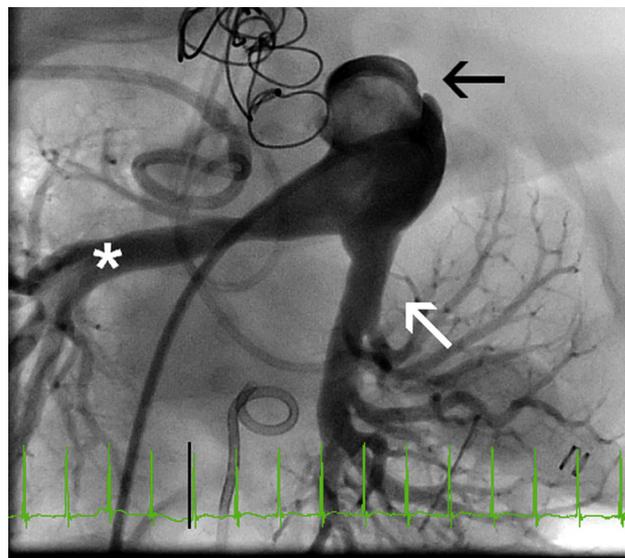
Figure 17 MPA angiography performed with 40° of caudal angulation outlines the PA bifurcation in detail. The homograft PV is seen "en face" (*black arrow*), there is no significant stenosis in the LPA (*white arrow*), and there is moderate stenosis in the RPA (*asterisk*).

precise delineation of the 3D anatomy of vascular structures outside the heart with rapid image processing and reduction of the amount of contrast and ionizing radiation used compared with those of multiple biplane angiograms in various projections.[186]

PAs. Depending on the findings at the time of hemodynamic assessment and on the results of prior imaging studies, pulmonary angiography may be performed selectively in each branch or in the MPA.[187] To evaluate the PA bifurcation and proximal branch PAs the AP camera is positioned as perpendicular as possible to the bifurcation, which is achieved with either cranial angulation (20°–30°) or extreme caudal angulation (35°–45°), depending on the orientation of the bifurcation within the chest (Figure 17). The distal PAs can be assessed with straight AP and lateral projections. To open the bifurcation of the right middle and lower lobes, 20° of caudal angulation in the lateral camera can be applied. In patients with arborization abnormalities, selective distal branch or segmental pulmonary angiography is recommended with variable angulation.

PR. There is no standard angiographic classification of PR severity. Patients with significant PR will have opacification of the right ventricle during pulmonary angiography. However, the presence of a catheter crossing the PV tends to artificially enhance the degree of regurgitation. Increased PA pulsatility with significant change in vessel dimension from systole to diastole is seen in patients with severe PR. Similarly, early diastolic pressure equilibration in the central PAs and the RV is indicative of significant PR.

Right Ventricle. i. Size.–Although right heart size is poorly assessed by x-ray angiography, it provides a gross qualitative estimate. To best visualize the RVOT, a mild degree (15°–20°) of cranial angulation is used in the AP camera.[187,188]

ii. Function.–Assessment of RV function is only qualitative given that its complex shape limits the ability to use geometric models to estimate volumes from biplane images.
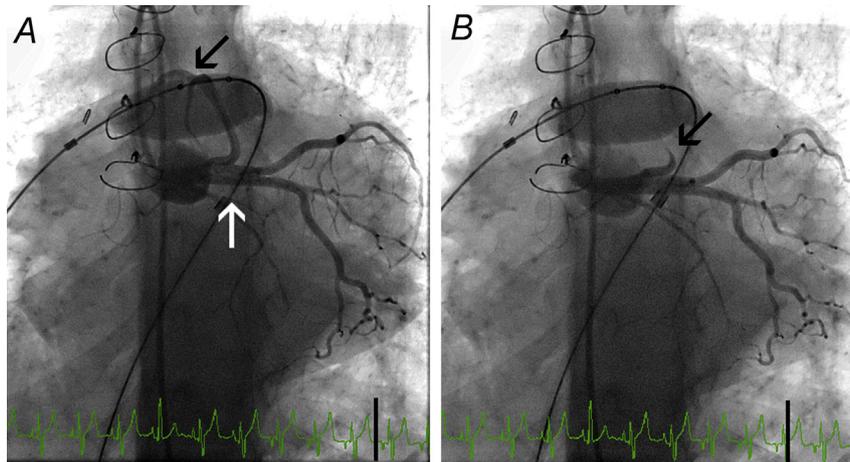
Figure 18 Coronary angiography performed on same patient as in Figure 17, during balloon compliance testing of a right ventricle–to–PA homograft. The patient has repaired TOF and single left coronary artery (*white arrow*) with right coronary artery (RCA) crossing the RVOT. Angiography is performed in the AP projection with extreme caudal angulation. **(A)** At the start of the balloon inflation, there is no evidence of obstruction of coronary flow (*black arrow*). **(B)** With the balloon inflated, further there is complete occlusion of RCA flow. Percutaneous PV implantation is therefore contraindicated in this patient.

Aortic Valve, Root, and Ascending Aorta. Aortic root angiography is standard in patients with repaired TOF. This allows demonstration of arch sidedness, aortic root and ascending aorta dimensions, coronary origins and course, AR, presence of aortopulmonary collateral vessels, or residual flow through prior surgical shunts.

Other Cardiovascular Issues. i. Coronary Arteries.—Selective coronary angiography is recommended in most patients with repaired TOF unless the vessels are clearly delineated by aortography. Patients with abnormal anatomic patterns that may have been altered at the time of prior surgical intervention require selective coronary angiography. Conal branches may have been disrupted and retrograde filling by collateral vessels can be seen in this setting. Detailed anatomic definition of the proximal course is needed in all patients who are being considered for percutaneous PV implantation or RV-to-PA conduit stenting. When in doubt, selective coronary angiography during simultaneous balloon dilation of the RVOT is performed to determine the risk for coronary compression with conduit expansion (Figure 18).[189,190]

ii. Aortopulmonary Collateral Vessels.—Once the collateral vessels are identified by aortography selective angiography in straight AP and lateral projections is performed. The levophase allows demonstration of the pulmonary venous return, the presence of any atrial-level shunt, and qualitative evaluation of LV function. In patients with discontinuity or atresia of a PA branch, anatomic definition of the atretic vessel is needed for surgical planning. If the vessel does not fill via aortopulmonary collateral flow, a pulmonary venous wedge injection is performed. This is best done in the lower lobe pulmonary vein.[187,188]

Noncardiac Findings. The relationship of the PAs to the airway can be appreciated on biplane angiography. Motion of the diaphragms can be assessed on fluoroscopy with the patient breathing spontaneously. Three-dimensional rotational angiography provides useful information on surrounding soft tissues in the tomographic volume sets that are generated. This may be relevant when associated vascular compression of the airway or potential erosion is suspected.

d. Standard Protocol

Patient Preparation. Before cardiac catheterization, patients undergo a thorough noninvasive evaluation to ensure an indication for x-ray angiography and refine the clinical questions for the test. This includes a thorough review of the patient's medical and surgical history, including any prior cardiac catheterizations, as well as other imaging studies performed. The sedation strategy for the procedure is then determined on the basis of the patient's hemodynamic, airway, and respiratory status as well as the nature of the catheterization procedure. General anesthesia is usually required when planning complex catheter interventions such as multiple PA balloon angioplasties or percutaneous PV implantation. Patients on anticoagulation medications should have these discontinued before the procedure, and those receiving warfarin may need to transition to heparin or enoxaparin.

In a stable patient undergoing diagnostic catheterization, it is possible to use minimal sedation and local anesthesia. However, the frequency of these procedures has declined significantly as most cardiac catheterizations now include a therapeutic intervention. All patients receive peripheral intravenous cannulas for hydration and administration of medications and are attached to cardiorespiratory monitors. Vascular access is obtained percutaneously using sterile technique. As mentioned earlier, it is standard to perform angiography in the biplane projection using a power injector at a rate of 1 to 2 mL/kg/sec (generally up to 40 mL).[187]

e. Recommendations

We recommend x-ray angiography for the assessment of critically ill patients or when noninvasive methods either cannot be performed or have failed to provide satisfactory data. Selective coronary angiography should be considered before cardiac and noncardiac procedures in adult patients at risk for coronary artery disease.

10. MULTIMODALITY APPROACH

The discussion of imaging modalities in the previous sections demonstrates that no single test is capable of providing all necessary

Table 6 Recommended multimodality imaging surveillance frequency in repaired TOF

Modality	Age (y)				
	<2 y*	2–9	10–19	20–49	≥50
Echocardiography	12 mo	12 mo	24 mo	24 mo	24 mo
CMR	Not recommended routinely; ordered to address specific questions not answered by echocardiography		• 36 mo in stable patients • 12 mo if moderate (≥150 mL/m^2) or progressive (increase of >25 mL/m^2) RV dilatation or dysfunction (RV EF ≤ 48% or ≥6% decrease in EF)		
CT	Not recommended routinely; ordered when CMR is indicated but cannot be performed (e.g., metallic artifacts or contraindications to CMR)				
Lung perfusion scan	If predicted RV systolic pressure 60% systemic or smallest branch PA diameter Z score < −2.5; in patients ≥10 y of age, consider CMR flow measurements				
X-ray angiography	Not recommended routinely[†]; ordered when noninvasive methods either cannot be performed or have failed to provide satisfactory diagnostic data				Coronary angiography when clinically indicated
Chest radiography	Not recommended routinely; may be ordered for evaluation of stent integrity				

*After the first postoperative outpatient evaluation.
[†]Integral part of an interventional catheterization procedure.

Table 7 Comparison of imaging modalities

Characteristic	Echocardiography	CMR	CT	Nuclear scintigraphy
Availability	++++	++	++	+++
Portability	++++	−	−	−
Cost (relative value units)*	9.11[†]	22.51[‡]	14.39[§]	13.59[‖]
Radiation risk	−	−	++++	++++
Artifacts from stainless-steel implants	+	+++	+	−
Sedation requirements in young children	++	++++	+++	++
Spatial resolution (mm)	<1	<1–2	<1	5–10
Temporal resolution (msec)	20	30	75–175	−[¶]
RV size/function	++	++++	+++	+
RV pressure	+++	+	+	−
TR severity	+++	+++	−	−
Mechanism of TR	++++	++	−	−
PR severity	++	++++	−	−
Branch PAs flow quantification	−	+++	−	++++
LV size/function	+++	++++	+++	++
Coronary origins and proximal course	++	+++	++++	−
Aortic dimensions	+++	++++	++++	−
Residual shunts	+++	+++	+	−
Pulmonary-to-systemic flow ratio	+	++++	+[#]	+
Aortopulmonary collateral vessels	−	+++	+++	−
Myocardial viability	+	++++	+	+++

Modified from Prakash et al.[9]
*From Centers for Medicare and Medicaid Services, National Physician Fee Schedule (http://www.cms.hhs.gov/PFSlookup/03_PFS_Document.asp).
[†]Sum of relative value units for Current Procedural Terminology (CPT) codes 93303, 93325 and 93320.
[‡]CPT code 75562.
[§]CPT code 71275.
[‖]CPT code 78465.
[¶]Temporal resolution for nuclear techniques is variable and depends on the radiotracer and counts.
[#]When measurement of ventricular stroke volume differential is physiologically appropriate.

diagnostic information in all clinical circumstances relevant to patients with repaired TOF. Therefore, a multimodality approach that takes into account patient-specific considerations, the strengths and weaknesses of each modality (Table 7), and institutional resources and expertise is recommended.[9]

Echocardiography is the primary imaging modality used in the evaluation of patients with repaired TOF during the first decade of life and should always be performed before other modalities are used. CMR is performed in this age group only when clinical or echocardiographic findings are concerning for important anatomic or hemodynamic abnormalities requiring therapeutic intervention. Reasons for not routinely using CMR in patients <8 to 10 years of age include the following: (1) most patients are clinically well during the first several years after repair, and RV size and function uncommonly reach severe levels of abnormalities, and (2) most young patients cannot cooperate with the test without sedation. As noted in the section on echocardiography, several recent publications have provided echocardiographic thresholds that can be used to identify young patients requiring further evaluation by CMR. Cardiovascular CT is rarely indicated in this age group except in patients with pacemakers or defibrillators who require quantification of RV size and function. Nuclear lung perfusion scanning is performed to quantify pulmonary perfusion, but the number of repeat scans should be kept to a minimum given the risk for cancer related to radiation exposure. Cardiac catheterization is typically performed for therapeutic interventions such as branch PA dilation or stenting, PV insertion, or occlusion of a residual shunt.

Once patients reach 8 to 10 years of age, the role of CMR increases, and the test becomes routine for surveillance of PR, RV size and function, differential PA flow, anatomic abnormalities such as RVOT aneurysm and aortic dilatation, and myocardial viability. Echocardiography continues to play an important role and is a vital adjunct to CMR for assessing TR and estimating RV and PA pressures. However, the diagnostic capabilities of echocardiography become more constrained by declining acoustic windows as patients' body sizes increase. The roles of other modalities also evolve with age. Cardiovascular CT continues to be used only when CMR is contraindicated, nuclear lung perfusion scan can be replaced by CMR flow measurements, and cardiac catheterization is predominantly used for therapy.

As patient age advances, clinical concerns become more complex, with increased prevalence of coronary artery disease and noncardiac comorbidities. These concerns influence the multimodality approach in this age group with an emphasis on assessment of the coronary circulation for acquired disease in addition to the other abnormalities related to TOF repair. As such, coronary CTA and x-ray angiography assume an important role in anatomic evaluation of the coronary arteries, nuclear imaging is used for assessment of myocardial ischemia, and CMR is used for evaluation of myocardial perfusion and viability.

A rational multimodality approach to outpatient surveillance of patients with repaired TOF takes into account all of the aforementioned considerations. A particular challenge in this population is the paucity of data on rates of progression of specific abnormalities such as RV dilatation and dysfunction. Specifically, we lack knowledge of predictors of rapid deterioration versus stable course of clinically important parameters. Therefore, little information exists to inform the frequency of testing. This gap in knowledge is particularly glaring in an era of increased awareness of resource utilization. With this background in mind, Table 6 represents a consensus recommendation for multimodality imaging in clinically stable patients with repaired TOF (level of evidence C).

NOTICE AND DISCLAIMER

This report is made available by the ASE as a courtesy reference source for its members. This report contains recommendations only and should not be used as the sole basis to make medical practice decisions or for disciplinary action against any employee. The statements and recommendations contained in this report are based primarily on the opinions of experts, rather than on scientifically verified data. The ASE makes no express or implied warranties regarding the completeness or accuracy of the information in this report, including the warranty of merchantability or fitness for a particular purpose. In no event shall the ASE be liable to you, your patients, or any other third parties for any decision made or action taken by you or such other parties in reliance on this information. Nor does your use of this information constitute the offering of medical advice by the ASE or create any physician-patient relationship between the ASE and your patients or anyone else.

REFERENCES

1. Hoffman JI, Kaplan S. The incidence of congenital heart disease. J Am Coll Cardiol 2002;39:1890-900.
2. Hamilton BE, Hoyert DL, Martin JA, Strobino DM, Guyer B. Annual summary of vital statistics: 2010-2011. Pediatrics 2013;131:548-58.
3. Al Habib HF, Jacobs JP, Mavroudis C, Tchervenkov CI, O'Brien SM, Mohammadi S, et al. Contemporary patterns of management of tetralogy of Fallot: data from the Society of Thoracic Surgeons database. Ann Thorac Surg 2010;90:813-9.
4. Chiu SN, Wang JK, Chen HC, Lin MT, Wu ET, Chen CA, et al. Long-term survival and unnatural deaths of patients with repaired tetralogy of Fallot in an Asian cohort. Circ Cardiovasc Qual Outcomes 2012;5:120-5.
5. Marelli AJ, Mackie AS, Ionescu-Ittu R, Rahme E, Pilote L. Congenital heart disease in the general population: changing prevalence and age distribution. Circulation 2007;115:163-72.
6. Le Gloan L, Guerin P, Mercier LA, Abbey S, Dore A, Marcotte F, et al. Clinical assessment of arrhythmias in tetralogy of Fallot. Expert Rev Cardiovasc Ther 2010;8:189-97.
7. Khairy P, Aboulhosn J, Gurvitz MZ, Opotowsky AR, Mongeon FP, Kay J, et al. Arrhythmia burden in adults with surgically repaired tetralogy of Fallot: a multi-institutional study. Circulation 2010;122:868-75.
8. Nollert G, Fischlein T, Bouterwek S, Bohmer C, Dewald O, Kreuzer E, et al. Long-term results of total repair of tetralogy of Fallot in adulthood: 35 years follow-up in 104 patients corrected at the age of 18 or older. Thorac Cardiovasc Surg 1997;45:178-81.
9. Prakash A, Powell AJ, Geva T. Multimodality noninvasive imaging for assessment of congenital heart disease. Circ Cardiovasc Imaging 2010; 3:112-25.
10. Kilner PJ, Geva T, Kaemmerer H, Trindade PT, Schwitter J, Webb GD. Recommendations for cardiovascular magnetic resonance in adults with congenital heart disease from the respective working groups of the European Society of Cardiology. Eur Heart J 2010;31:794-805.
11. Geva T. Repaired tetralogy of Fallot: the roles of cardiovascular magnetic resonance in evaluating pathophysiology and for pulmonary valve replacement decision support. J Cardiovasc Magn Reson 2011;13:9.
12. Warnes CA, Williams RG, Bashore TM, Child JS, Connolly HM, Dearani JA, et al. ACC/AHA 2008 guidelines for the management of adults with congenital heart disease: a report of the American College of Cardiology/American Heart Association Task Force on Practice Guidelines (Writing Committee to Develop Guidelines on the Management of Adults with Congenital Heart Disease). Circulation 2008;118: e714-833.
13. Blalock A, Taussig HB. Landmark article May 19 1945: the surgical treatment of malformations of the heart in which there is pulmonary stenosis or pulmonary atresia. JAMA 1984;251:2123-38.

14. Karpawich PP, Bush CP, Antillon JR, Amato JJ, Marbey ML, Agarwal KC. Modified Blalock-Taussig shunt in infants and young children. Clinical and catheterization assessment. J Thorac Cardiovasc Surg 1985;89:275-9.

15. Sabri MR, Sholler G, Hawker R, Nunn G. Branch pulmonary artery growth after Blalock-Taussig shunts in tetralogy of Fallot and pulmonary atresia with ventricular septal defect: a retrospective, echocardiographic study. Pediatr Cardiol 1999;20:358-63.

16. Alfieri O, Locatelli G, Bianchi T, Vanini V, Parenzan L. Repair of tetralogy of Fallot after Waterston anastomosis. J Thorac Cardiovasc Surg 1979;77:826-31.

17. Daniel FJ, Clarke CP, Richardson JP, Westlake GW, Jones PG. An evaluation of Potts' aortopulmonary shunt for palliation of cyanotic heart disease. Thorax 1976;31:394-7.

18. Yamaki S. Pulmonary vascular disease in shunted and nonshunted patients with tetralogy of Fallot. Tohoku J Exp Med 1990;162:109-19.

19. Gelb BD. Molecular genetics of congenital heart disease. Curr Opin Cardiol 1997;12:321-8.

20. Ito M, Kikuchi S, Hachiro Y, Abe T. Anomalous subaortic position of the brachiocephalic vein associated with tetralogy of Fallot. Ann Thorac Cardiovasc Surg 2011;7:106-8.

21. Chaturvedi R, Mikailian H, Freedom RM. Crossed pulmonary arteries in tetralogy of Fallot. Cardiol Young 2005;15:537.

22. Eyskens B, Brown SC, Claus P, Dymarkowski S, Gewillig M, Bogaert J, et al. The influence of pulmonary regurgitation on regional right ventricular function in children after surgical repair of tetralogy of Fallot. Eur J Echocardiogr 2010;11:341-5.

23. Rudski LG, Lai WW, Afilalo J, Hua L, Handschumacher MD, Chandrasekaran K, et al. Guidelines for the echocardiographic assessment of the right heart in adults: a report from the American Society of Echocardiography endorsed by the European Association of Echocardiography, a registered branch of the European Society of Cardiology, and the Canadian Society of Echocardiography. J Am Soc Echocardiogr 2010;23:685-713.

24. Baumgartner H, Hung J, Bermejo J, Chambers JB, Evangelista A, Griffin BP, et al. Echocardiographic assessment of valve stenosis: EAE/ASE recommendations for clinical practice. J Am Soc Echocardiogr 2009;22:1-23.

25. Redington AN. Determinants and assessment of pulmonary regurgitation in tetralogy of Fallot: practice and pitfalls. Cardiol Clin 2006;24:631-9.

26. Gatzoulis MA, Balaji S, Webber SA, Siu SC, Hokanson JS, Poile C, et al. Risk factors for arrhythmia and sudden cardiac death late after repair of tetralogy of Fallot: a multicentre study. Lancet 2000;356:975-81.

27. Lu JC, Cotts TB, Agarwal PP, Attili AK, Dorfman AL. Relation of right ventricular dilation, age of repair, and restrictive right ventricular physiology with patient-reported quality of life in adolescents and adults with repaired tetralogy of Fallot. Am J Cardiol 2010;106:1798-802.

28. Therrien J, Siu SC, McLaughlin PR, Liu PP, Williams WG, Webb GD. Pulmonary valve replacement in adults late after repair of tetralogy of Fallot: are we operating too late? J Am Coll Cardiol 2000;36:1670-5.

29. Warnes CA. Adult congenital heart disease importance of the right ventricle. J Am Coll Cardiol 2009;54:1903-10.

30. Kilner PJ, Balossino R, Dubini G, Babu-Narayan SV, Taylor AM, Pennati G, et al. Pulmonary regurgitation: the effects of varying pulmonary artery compliance, and of increased resistance proximal or distal to the compliance. Int J Cardiol 2009;133:157-66.

31. Zoghbi WA, Enriquez-Sarano M, Foster E, Grayburn PA, Kraft CD, Levine RA, et al. Recommendations for evaluation of the severity of native valvular regurgitation with two-dimensional and Doppler echocardiography. J Am Soc Echocardiogr 2003;16:777-802.

32. Li W, Davlouros PA, Kilner PJ, Pennell DJ, Gibson D, Henein MY, et al. Doppler-echocardiographic assessment of pulmonary regurgitation in adults with repaired tetralogy of Fallot: comparison with cardiovascular magnetic resonance imaging. Am Heart J 2004;147:165-72.

33. Puchalski MD, Askovich B, Sower CT, Williams RV, Minich LL, Tani LY. Pulmonary regurgitation: determining severity by echocardiography and magnetic resonance imaging. Congenit Heart Dis 2008;3:168-75.

34. Renella P, Aboulhosn J, Lohan DG, Jonnala P, Finn JP, Satou GM, et al. Two-dimensional and Doppler echocardiography reliably predict severe pulmonary regurgitation as quantified by cardiac magnetic resonance. J Am Soc Echocardiogr 2010;23:880-6.

35. Silversides CK, Veldtman GR, Crossin J, Merchant N, Webb GD, McCrindle BW, et al. Pressure half-time predicts hemodynamically significant pulmonary regurgitation in adult patients with repaired tetralogy of Fallot. J Am Soc Echocardiogr 2003;16:1057-62.

36. Fukuda S, Song JM, Gillinov AM, McCarthy PM, Daimon M, Kongsaerepong V, et al. Tricuspid valve tethering predicts residual tricuspid regurgitation after tricuspid annuloplasty. Circulation 2005;111:975-9.

37. Fukuda S, Gillinov AM, Song JM, Daimon M, Kongsaerepong V, Thomas JD, et al. Echocardiographic insights into atrial and ventricular mechanisms of functional tricuspid regurgitation. Am Heart J 2006;152:1208-14.

38. Grossmann G, Stein M, Kochs M, Hoher M, Koenig W, Hombach V, et al. Comparison of the proximal flow convergence method and the jet area method for the assessment of the severity of tricuspid regurgitation. Eur Heart J 1998;19:652-9.

39. Alghamdi MH, Grosse-Wortmann L, Ahmad N, Mertens L, Friedberg MK. Can simple echocardiographic measures reduce the number of cardiac magnetic resonance imaging studies to diagnose right ventricular enlargement in congenital heart disease? J Am Soc Echocardiogr 2012;25:518-23.

40. Puchalski MD, Williams RV, Askovich B, Minich LL, Mart C, Tani LY. Assessment of right ventricular size and function: echo versus magnetic resonance imaging. Congenit Heart Dis 2007;2:27-31.

41. Lai WW, Gauvreau K, Rivera ES, Saleeb S, Powell AJ, Geva T. Accuracy of guideline recommendations for two-dimensional quantification of the right ventricle by echocardiography. Int J Cardiovasc Imaging 2008;24:691-8.

42. Jenkins C, Chan J, Bricknell K, Strudwick M, Marwick TH. Reproducibility of right ventricular volumes and ejection fraction using real-time three-dimensional echocardiography: comparison with cardiac MRI. Chest 2007;131:1844-51.

43. Lu X, Nadvoretskiy V, Bu L, Stolpen A, Ayres N, Pignatelli RH, Kovalchin JP, Grenier M, Klas B, Ge S. Accuracy and reproducibility of real-time three-dimensional echocardiography for assessment of right ventricular volumes and ejection fraction in children. J Am Soc Echocardiogr 2008;21:84-9.

44. Grewal J, Majdalany D, Syed I, Pellikka P, Warnes CA. Three-dimensional echocardiographic assessment of right ventricular volume and function in adult patients with congenital heart disease: comparison with magnetic resonance imaging. J Am Soc Echocardiogr 2010;23:127-33.

45. Dragulescu A, Grosse-Wortmann L, Fackoury C, Riffle S, Waiss M, Jaeggi E, et al. Echocardiographic assessment of right ventricular volumes after surgical repair of tetralogy of Fallot: clinical validation of a new echocardiographic method. J Am Soc Echocardiogr 2011;24:1191-8.

46. Helbing WA, Bosch HG, Maliepaard C, Rebergen SA, van der Geest RJ, Hansen B, et al. Comparison of echocardiographic methods with magnetic resonance imaging for assessment of right ventricular function in children. Am J Cardiol 1995;76:589-94.

47. Shimada YJ, Shiota M, Siegel RJ, Shiota T. Accuracy of right ventricular volumes and function determined by three-dimensional echocardiography in comparison with magnetic resonance imaging: a meta-analysis study. J Am Soc Echocardiogr 2010;23:943-53.

48. Renella P, Marx GR, Gauvreau K, Zhou J, Geva T. 3D echocardiographic assessment of right ventricular size and function in children: feasibility and reproducibility. J Am Soc Echocardiogr 2011;24.

49. Muzzarelli S, Ordovas KG, Cannavale G, Meadows AK, Higgins CB. Tetralogy of Fallot: impact of the excursion of the interventricular septum on left ventricular systolic function and fibrosis after surgical repair. Radiology 2011;259:375-83.

50. Geva T, Sandweiss BM, Gauvreau K, Lock JE, Powell AJ. Factors associated with impaired clinical status in long-term survivors of tetralogy of Fallot repair evaluated by magnetic resonance imaging. J Am Coll Cardiol 2004;43:1068-74.

51. Davlouros PA, Kilner PJ, Hornung TS, Li W, Francis JM, Moon JC, et al. Right ventricular function in adults with repaired tetralogy of Fallot assessed with cardiovascular magnetic resonance imaging: detrimental role of right ventricular outflow aneurysms or akinesia and adverse right-to-left ventricular interaction. J Am Coll Cardiol 2002;40: 2044-52.

52. Thambo JB, De Guillebon M, Dos Santos P, Xhaet O, Ploux S, Iriart X, et al. Electrical dyssynchrony and resynchronization in tetralogy of Fallot. Heart Rhythm 2011;8:909-14.

53. Mueller M, Rentzsch A, Hoetzer K, Raedle-Hurst T, Boettler P, Stiller B, et al. Assessment of interventricular and right-intraventricular dyssynchrony in patients with surgically repaired tetralogy of Fallot by two-dimensional speckle tracking. Eur J Echocardiogr 2010;11: 786-92.

54. Anavekar NS, Gerson D, Skali H, Kwong RY, Yucel EK, Solomon SD. Two-dimensional assessment of right ventricular function: an echocardiographic-MRI correlative study. Echocardiography 2007;24: 452-6.

55. Wang J, Prakasa K, Bomma C, Tandri H, Dalal D, James C, et al. Comparison of novel echocardiographic parameters of right ventricular function with ejection fraction by cardiac magnetic resonance. J Am Soc Echocardiogr 2007;20:1058-64.

56. Srinivasan C, Sachdeva R, Morrow WR, Greenberg SB, Vyas HV. Limitations of standard echocardiographic methods for quantification of right ventricular size and function in children and young adults. J Ultrasound Med 2011;30:487-93.

57. Gleason WL, Braunwald E. Studies on the first derivative of the ventricular pressure pulse in man. J Clin Invest 1962;41:80-91.

58. Duan YY, Harada K, Toyono M, Ishii H, Tamura M, Takada G. Effects of acute preload reduction on myocardial velocity during isovolumic contraction and myocardial acceleration in pediatric patients. Pediatr Cardiol 2006;27:32-6.

59. Kjaergaard J, Snyder EM, Hassager C, Oh JK, Johnson BD. Impact of preload and afterload on global and regional right ventricular function and pressure: a quantitative echocardiography study. J Am Soc Echocardiogr 2006;19:515-21.

60. Vogel M, Schmidt MR, Kristiansen SB, Cheung M, White PA, Sorensen K, et al. Validation of myocardial acceleration during isovolumic contraction as a novel noninvasive index of right ventricular contractility: comparison with ventricular pressure-volume relations in an animal model. Circulation 2002;105:1693-9.

61. Tei C, Dujardin KS, Hodge DO, Bailey KR, McGoon MD, Tajik AJ, et al. Doppler echocardiographic index for assessment of global right ventricular function. J Am Soc Echocardiogr 1996;9:838-47.

62. Cetin I, Tokel K, Varan B, Orun U, Aslamaci S. Evaluation of right ventricular function by using tissue Doppler imaging in patients after repair of tetralogy of Fallot. Echocardiography 2009;26:950-7.

63. Yasuoka K, Harada K, Toyono M, Tamura M, Yamamoto F. Tei index determined by tissue Doppler imaging in patients with pulmonary regurgitation after repair of tetralogy of Fallot. Pediatr Cardiol 2004;25:131-6.

64. Abd El Rahman MY, Abdul-Khaliq H, Vogel M, Alexi-Meskischvili V, Gutberlet M, Hetzer R, et al. Value of the new Doppler-derived myocardial performance index for the evaluation of right and left ventricular function following repair of tetralogy of Fallot. Pediatr Cardiol 2002;23:502-7.

65. Schwerzmann M, Samman AM, Salehian O, Holm J, Provost Y, Webb GD, et al. Comparison of echocardiographic and cardiac magnetic resonance imaging for assessing right ventricular function in adults with repaired tetralogy of Fallot. Am J Cardiol 2007;99:1593-7.

66. Kjaergaard J, Petersen CL, Kjaer A, Schaadt BK, Oh JK, Hassager C. Evaluation of right ventricular volume and function by 2D and 3D echocardiography compared to MRI. Eur J Echocardiogr 2006;7:430-8.

67. Kaul S, Tei C, Hopkins JM, Shah PM. Assessment of right ventricular function using two-dimensional echocardiography. Am Heart J 1984;107: 526-31.

68. Urheim S, Cauduro S, Frantz R, McGoon M, Belohlavek M, Green T, et al. Relation of tissue displacement and strain to invasively determined right ventricular stroke volume. Am J Cardiol 2005;96:1173-8.

69. Bonnemains L, Stos B, Vaugrenard T, Marie PY, Odille F, Boudjemline Y. Echocardiographic right ventricle longitudinal contraction indices cannot predict ejection fraction in post-operative Fallot children. Eur Heart J Cardiovasc Imaging 2012;13:235-42.

70. Koestenberger M, Nagel B, Ravekes W, Everett AD, Stueger HP, Heinzl B, et al. Tricuspid annular plane systolic excursion and right ventricular ejection fraction in pediatric and adolescent patients with tetralogy of Fallot, patients with atrial septal defect, and age-matched normal subjects. Clin Res Cardiol 2011;100:67-75.

71. Morcos P, Vick GW III, Sahn DJ, Jerosch-Herold M, Shurman A, Sheehan FH. Correlation of right ventricular ejection fraction and tricuspid annular plane systolic excursion in tetralogy of Fallot by magnetic resonance imaging. Int J Cardiovasc Imaging 2009;25:263-70.

72. Koestenberger M, Ravekes W, Everett AD, Stueger HP, Heinzl B, Gamillscheg A, et al. Right ventricular function in infants, children and adolescents: reference values of the tricuspid annular plane systolic excursion (TAPSE) in 640 healthy patients and calculation of Z score values. J Am Soc Echocardiogr 2009;22:715-9.

73. Koestenberger M, Nagel B, Ravekes W, Everett AD, Stueger HP, Heinzl B, et al. Systolic right ventricular function in pediatric and adolescent patients with tetralogy of Fallot: echocardiography versus magnetic resonance imaging. J Am Soc Echocardiogr 2011;24:45-52.

74. Pavlicek M, Wahl A, Rutz T, de Marchi SF, Hille R, Wustmann K, et al. Right ventricular systolic function assessment: rank of echocardiographic methods vs. cardiac magnetic resonance imaging. Eur J Echocardiogr 2011;12:871-80.

75. Kutty S, Zhou J, Gauvreau K, Trincado C, Powell AJ, Geva T. Regional dysfunction of the right ventricular outflow tract reduces the accuracy of Doppler tissue imaging assessment of global right ventricular systolic function in patients with repaired tetralogy of Fallot. J Am Soc Echocardiogr 2011;24:637-43.

76. Gatzoulis MA, Clark AL, Cullen S, Newman CG, Redington AN. Right ventricular diastolic function 15 to 35 years after repair of tetralogy of Fallot. Restrictive physiology predicts superior exercise performance. Circulation 1995;91:1775-81.

77. Cullen S, Shore D, Redington A. Characterization of right ventricular diastolic performance after complete repair of tetralogy of Fallot. Restrictive physiology predicts slow postoperative recovery. Circulation 1995;91: 1782-9.

78. van den Berg J, Wielopolski PA, Meijboom FJ, Witsenburg M, Bogers AJ, Pattynama PM, et al. Diastolic function in repaired tetralogy of Fallot at rest and during stress: assessment with MR imaging. Radiology 2007; 243:212-9.

79. Hui W, Abd El Rahman MY, Dsebissowa F, Rentzsch A, Gutberlet M, Alexi-Meskishvili V, et al. Quantitative analysis of right atrial performance after surgical repair of tetralogy of Fallot. Cardiol Young 2004; 14:520-6.

80. Ghai A, Silversides C, Harris L, Webb GD, Siu SC, Therrien J. Left ventricular dysfunction is a risk factor for sudden cardiac death in adults late after repair of tetralogy of Fallot. J Am Coll Cardiol 2002;40:1675-80.

81. Knauth AL, Gauvreau K, Powell AJ, Landzberg MJ, Walsh EP, Lock JE, et al. Ventricular size and function assessed by cardiac MRI predict major adverse clinical outcomes late after tetralogy of Fallot repair. Heart 2008; 94:211-6.

82. Colan SD, Shirali G, Margossian R, Gallagher D, Altmann K, Canter C, et al. The Ventricular Volume Variability Study of the Pediatric Heart Network: study design and impact of beat averaging and variable type on the reproducibility of echocardiographic measurements in children with chronic dilated cardiomyopathy. J Am Soc Echocardiogr 2012;25: 842-54.

83. Diller GP, Kempny A, Liodakis E, Alonso-Gonzalez R, Inuzuka R, Uebing A, et al. Left ventricular longitudinal function predicts life-threatening ventricular arrhythmia and death in adults with repaired tetralogy of Fallot. Circulation 2012;125:2440-6.

84. Brili S, Stamatopoulos I, Barbetseas J, Chrysohoou C, Alexopoulos N, Misailidou M, et al. Usefulness of dobutamine stress echocardiography with tissue Doppler imaging for the evaluation and follow-up of patients

with repaired tetralogy of Fallot. J Am Soc Echocardiogr 2008;21: 1093-8.

85. Baspinar O, Alehan D. Dobutamine stress echocardiography in the evaluation of cardiac haemodynamics after repair of tetralogy of Fallot in children: negative effects of pulmonary regurgitation. Acta Cardiol 2006;61: 279-83.

86. Dodds GA, Warnes CA, Danielson GK. Aortic valve replacement after repair of pulmonary atresia and ventricular septal defect or tetralogy of Fallot. J Thorac Cardiovasc Surg 1997;113:736-41.

87. Niwa K. Aortic root dilatation in tetralogy of Fallot long-term after repair—histology of the aorta in tetralogy of Fallot: evidence of intrinsic aortopathy. Int J Cardiol 2005;103:117-9.

88. Lopez L, Colan SD, Frommelt PC, Ensing GJ, Kendall K, Younoszai AK, et al. Recommendations for quantification methods during the performance of a pediatric echocardiogram: a report from the Pediatric Measurements Writing Group of the American Society of Echocardiography Pediatric and Congenital Heart Disease Council. J Am Soc Echocardiogr 2010;23:465-95.

89. Hiratzka LF, Bakris GL, Beckman JA, Bersin RM, Carr VF, Casey DE, et al. 2010 ACCF/AHA/AATS/ACR/ASA/SCA/SCAI/SIR/STS/SVM guidelines for the diagnosis and management of patients with thoracic aortic disease. A report of the American College of Cardiology Foundation/American Heart Association Task Force on Practice Guidelines, American Association for Thoracic Surgery, American College of Radiology, American Stroke Association, Society of Cardiovascular Anesthesiologists, Society for Cardiovascular Angiography and Interventions, Society of Interventional Radiology, Society of Thoracic Surgeons, and Society for Vascular Medicine. J Am Coll Cardiol 2010;55:e27-129.

90. Haycock GB, Schwartz GJ, Wisotsky DH. Geometric method for measuring body surface area: a height-weight formula validated in infants, children, and adults. J Pediatr 1978;93:62-6.

91. DuBois D, DuBois E. A formula to estimate the approximate surface area if height and weight be known. Arch Intern Med 1916;17:863-71.

92. Lai WW, Geva T, Shirali GS, Frommelt PC, Humes RA, Brook MM, et al. Guidelines and standards for performance of a pediatric echocardiogram: a report from the Task Force of the Pediatric Council of the American Society of Echocardiography. J Am Soc Echocardiogr 2006;19: 1413-30.

93. Festa P, Ait-Ali L, Minichilli F, Kristo I, Deiana M, Picano E. A new simple method to estimate pulmonary regurgitation by echocardiography in operated Fallot: comparison with magnetic resonance imaging and performance test evaluation. J Am Soc Echocardiogr 2010;23:496-503.

94. Chessa M, Butera G, Carminati M. Intracardiac echocardiography during percutaneous pulmonary valve replacement. Eur Heart J 2008;29:2908.

95. Plein S, Bloomer TN, Ridgway JP, Jones TR, Bainbridge GJ, Sivananthan MU. Steady-state free precession magnetic resonance imaging of the heart: comparison with segmented k-space gradient-echo imaging. J Magn Reson Imaging 2011;14:230-6.

96. Babu-Narayan SV, Kilner PJ, Li W, Moon JC, Goktekin O, Davlouros PA, et al. Ventricular fibrosis suggested by cardiovascular magnetic resonance in adults with repaired tetralogy of Fallot and its relationship to adverse markers of clinical outcome. Circulation 2006;113:405-13.

97. Wald RM, Haber I, Wald R, Valente AM, Powell AJ, Geva T. Effects of regional dysfunction and late gadolinium enhancement on global right ventricular function and exercise capacity in patients with repaired tetralogy of Fallot. Circulation 2009;119:1370-7.

98. Helbing WA, de Roos A. Clinical applications of cardiac magnetic resonance imaging after repair of tetralogy of Fallot. Pediatr Cardiol 2000;21:70-9.

99. van Straten A, Vliegen HW, Hazekamp MG, Bax JJ, Schoof PH, Ottenkamp J, et al. Right ventricular function after pulmonary valve replacement in patients with tetralogy of Fallot. Radiology 2004;233: 824-9.

100. Vliegen HW, Van Straten A, De Roos A, Roest AA, Schoof PH, Zwinderman AH, et al. Magnetic resonance imaging to assess the hemodynamic effects of pulmonary valve replacement in adults late after repair of tetralogy of Fallot. Circulation 2002;106:1703-7.

101. Babu-Narayan SV, Gatzoulis MA. Management of adults with operated tetralogy of Fallot. Curr Treat Options Cardiovasc Med 2003;5:389-98.

102. Garg R, Powell AJ, Sena L, Marshall AC, Geva T. Effects of metallic implants on magnetic resonance imaging evaluation of Fontan palliation. Am J Cardiol 2005;95:688-91.

103. Sorrentino RA. A novel MRI-safe dual-chamber pacemaker system: its time has come. Heart Rhythm 2011;8:74-5.

104. Reiter T, Ritter O, Prince MR, Nordbeck P, Wanner C, Nagel E, et al. Minimizing risk of nephrogenic systemic fibrosis in cardiovascular magnetic resonance. J Cardiovasc Magn Reson 2012;14:31.

105. Sridharan S, Derrick G, Deanfield J, Taylor AM. Assessment of differential branch pulmonary blood flow: a comparative study of phase contrast magnetic resonance imaging and radionuclide lung perfusion imaging. Heart 2006;92:963-8.

106. Schievano S, Coats L, Migliavacca F, Norman W, Frigiola A, Deanfield J, et al. Variations in right ventricular outflow tract morphology following repair of congenital heart disease: implications for percutaneous pulmonary valve implantation. J Cardiovasc Magn Reson 2007;9:687-95.

107. Weber OM, Higgins CB. MR evaluation of cardiovascular physiology in congenital heart disease: flow and function. J Cardiovasc Magn Reson 2006;8:607-17.

108. Greil GF, Stuber M, Botnar RM, Kissinger KV, Geva T, Newburger JW, et al. Coronary magnetic resonance angiography in adolescents and young adults with Kawasaki disease. Circulation 2002;105:908-11.

109. Valverde I, Parish V, Hussain T, Rosenthal E, Beerbaum P, Krasemann T. Planning of catheter interventions for pulmonary artery stenosis: improved measurement agreement with magnetic resonance angiography using identical angulations. Catheter Cardiovasc Interv 2011;77: 400-8.

110. Nordmeyer J, Gaudin R, Tann OR, Lurz PC, Bonhoeffer P, Taylor AM, et al. MRI may be sufficient for noninvasive assessment of great vessel stents: an in vitro comparison of MRI, CT, and conventional angiography. AJR Am J Roentgenol 2010;195:865-71.

111. Wald RM, Redington AN, Pereira A, Provost YL, Paul NS, Oechslin EN, et al. Refining the assessment of pulmonary regurgitation in adults after tetralogy of Fallot repair: should we be measuring regurgitant fraction or regurgitant volume? Eur Heart J 2009;30:356-61.

112. Geva T, Gauvreau K, Powell AJ, Cecchin F, Rhodes J, Geva J, et al. Randomized trial of pulmonary valve replacement with and without right ventricular remodeling surgery. Circulation 2010;122:S201-8.

113. van der Hulst AE, Westenberg JJ, Kroft LJ, Bax JJ, Blom NA, de Roos A, et al. Tetralogy of Fallot: 3D velocity-encoded MR imaging for evaluation of right ventricular valve flow and diastolic function in patients after correction. Radiology 2010;256:724-34.

114. Norton KI, Tong C, Glass RB, Nielsen JC. Cardiac MR imaging assessment following tetralogy of Fallot repair. Radiographics 2006;26:197-211.

115. Samyn MM, Powell AJ, Garg R, Sena L, Geva T. Range of ventricular dimensions and function by steady-state free precession cine MRI in repaired tetralogy of Fallot: right ventricular outflow tract patch vs. conduit repair. J Magn Reson Imaging 2007;26:934-40.

116. Mooij CF, de Wit CJ, Graham DA, Powell AJ, Geva T. Reproducibility of MRI measurements of right ventricular size and function in patients with normal and dilated ventricles. J Magn Reson Imaging 2008;28:67-73.

117. Blalock SE, Banka P, Geva T, Powell AJ, Zhou J, Prakash A. Interstudy variability in cardiac magnetic resonance imaging measurements of ventricular volume, mass, and ejection fraction in repaired tetralogy of Fallot: a prospective observational study. J Magn Reson Imaging 2013;38:829-35.

118. Sarikouch S, Peters B, Gutberlet M, Leismann B, Kelter-Kloepping A, Koerperich H, et al. Sex-specific pediatric percentiles for ventricular size and mass as reference values for cardiac MRI: assessment by steady-state free-precession and phase-contrast MRI flow. Circ Cardiovasc Imaging 2010;3:65-76.

119. Valente AM, Gauvreau K, Assenza GE, Babu-Narayan SV, Schreier J, Gatzoulis M, et al. Contemporary predictors of death and sustained ventricular tachycardia in patients with repaired tetralogy of Fallot enrolled in the INDICATOR cohort. Heart. In press.

120. Kim RJ, Fieno DS, Parrish TB, Harris K, Chen EL, Simonetti O, et al. Relationship of MRI delayed contrast enhancement to irreversible injury, infarct age, and contractile function. Circulation 1999;100:1992-2002.

121. Gulati A, Jabbour A, Ismail TF, Guha K, Khwaja J, Raza S, et al. Association of fibrosis with mortality and sudden cardiac death in patients with non-ischemic dilated cardiomyopathy. JAMA 2013;309:896-908.

122. Valverde I, Parish V, Tzifa A, Head C, Sarikouch S, Greil G, et al. Cardiovascular MR dobutamine stress in adult tetralogy of Fallot: disparity between CMR volumetry and flow for cardiovascular function. J Magn Reson Imaging 2011;33:1341-50.

123. Parish V, Valverde I, Kutty S, Head C, Qureshi SA, Sarikouch S, et al. Dobutamine stress MRI in repaired tetralogy of Fallot with chronic pulmonary regurgitation a comparison with healthy volunteers. Int J Cardiol 2013;166:96-105.

124. Riesenkampff E, Mengelkamp L, Mueller M, Kropf S, Abdul-Khaliq H, Sarikouch S, et al. Integrated analysis of atrioventricular interactions in tetralogy of Fallot. Am J Physiol Heart Circ Physiol 2010;299: H364-71.

125. Luijnenburg SE, Peters RE, van der Geest RJ, Moelker A, Roos-Hesselink JW, de Rijke YB, et al. Abnormal right atrial and right ventricular diastolic function relate to impaired clinical condition in patients operated for tetralogy of Fallot. Int J Cardiol 2013;167:833-9.

126. Broberg CS, Aboulhosn J, Mongeon FP, Kay J, Valente AM, Khairy P, et al. Prevalence of left ventricular systolic dysfunction in adults with repaired tetralogy of Fallot. Am J Cardiol 2011;107:1215-20.

127. Darsee JR, Mikolich JR, Walter PF, Schlant RC. Paradoxical rise in left ventricular filling pressure in the dog during positive end-expiratory pressure ventilation. A reversed Bernheim effect. Circ Res 1981;49:1017-28.

128. Lurz P, Puranik R, Nordmeyer J, Muthurangu V, Hansen MS, Schievano S, et al. Improvement in left ventricular filling properties after relief of right ventricle to pulmonary artery conduit obstruction: contribution of septal motion and interventricular mechanical delay. Eur Heart J 2009;30:2266-74.

129. Powell AJ, Maier SE, Chung T, Geva T. Phase-velocity cine magnetic resonance imaging measurement of pulsatile blood flow in children and young adults: in vitro and in vivo validation. Pediatr Cardiol 2000;21: 104-10.

130. Potthast S, Mitsumori L, Stanescu LA, Richardson ML, Branch K, Dubinsky TJ, et al. Measuring aortic diameter with different MR techniques: comparison of three-dimensional (3D) navigated steady-state free-precession (SSFP), 3D contrast-enhanced magnetic resonance angiography (CE-MRA), 2D T2 black blood, and 2D cine SSFP. J Magn Reson Imaging 2010;31:177-84.

131. Kaiser T, Kellenberger CJ, Albisetti M, Bergstrasser E, Valsangiacomo Buechel ER. Normal values for aortic diameters in children and adolescents—assessment in vivo by contrast-enhanced CMR-angiography. J Cardiovasc Magn Reson 2008;10:56.

132. Schulz-Menger J, Bluemke DA, Bremerich J, Flamm SD, Fogel MA, Friedrich MG, et al. Standardized image interpretation and post processing in cardiovascular magnetic resonance: Society for Cardiovascular Magnetic Resonance (SCMR) Board of Trustees Task Force on Standardized Post Processing. J Cardiovasc Magn Reson 2013;15:35.

133. Lurz P, Coats L, Khambadkone S, Nordmeyer J, Boudjemline Y, Schievano S, et al. Percutaneous pulmonary valve implantation: impact of evolving technology and learning curve on clinical outcome. Circulation 2008;117:1964-72.

134. Atalay MK, Prince EA, Pearson CA, Chang KJ. The prevalence and clinical significance of noncardiac findings on cardiac MRI. AJR Am J Roentgenol 2011;196:W387-93.

135. Whitlock M, Garg A, Gelow J, Jacobson T, Broberg C. Comparison of left and right atrial volume by echocardiography versus cardiac magnetic resonance imaging using the area-length method. Am J Cardiol 2010; 106:1345-50.

136. Ginde AA, Foianini A, Renner DM, Valley M, Camargo CA Jr. Availability and quality of computed tomography and magnetic resonance imaging equipment in U.S. emergency departments. Acad Emerg Med 2008; 15:780-3.

137. Fuchs T, Kachelriess M, Kalender WA. Technical advances in multi-slice spiral CT. Eur J Radiol 2000;36:69-73.

138. Desjardins B, Kazerooni EA. ECG-gated cardiac CT. AJR Am J Roentgenol 2004;182:993-1010.

139. Einstein AJ, Elliston CD, Arai AE, Chen MY, Mather R, Pearson GD, et al. Radiation dose from single-heartbeat coronary CT angiography performed with a 320-detector row volume scanner. Radiology 2010; 254:698-706.

140. Gerber TC, Kuzo RS, Lane GE, O'Brien PC, Karstaedt N, Morin RL, et al. Image quality in a standardized algorithm for minimally invasive coronary angiography with multislice spiral computed tomography. J Comput Assist Tomogr 2003;27:62-9.

141. Moloo J, Shapiro MD, Abbara S. Cardiac computed tomography: technique and optimization of protocols. Semin Roentgenol 2008; 43:90-9.

142. Nicol ED, Gatzoulis M, Padley SP, Rubens M. Assessment of adult congenital heart disease with multi-detector computed tomography: beyond coronary lumenography. Clin Radiol 2007;62:518-27.

143. Pearce MS, Salotti JA, Little MP, McHugh K, Lee C, Kim KP, et al. Radiation exposure from CT scans in childhood and subsequent risk of leukaemia and brain tumours: a retrospective cohort study. Lancet 2012;380:499-505.

144. Brenner DJ, Doll R, Goodhead DT, Hall EJ, Land CE, Little JB, et al. Cancer risks attributable to low doses of ionizing radiation: assessing what we really know. Proc Natl Acad Sci U S A 2003;100:13761-6.

145. Fazel R, Krumholz HM, Wang Y, Ross JS, Chen J, Ting HH, et al. Exposure to low-dose ionizing radiation from medical imaging procedures. N Engl J Med 2009;361:849-57.

146. Kleinerman RA. Cancer risks following diagnostic and therapeutic radiation exposure in children. Pediatr Radiol 2006;36(suppl):121-5.

147. Brenner DJ. Estimating cancer risks from pediatric CT: going from the qualitative to the quantitative. Pediatr Radiol 2002;32:242-8.

148. Weisbord SD, Mor MK, Resnick AL, Hartwig KC, Palevsky PM, Fine MJ. Incidence and outcomes of contrast-induced AKI following computed tomography. Clin J Am Soc Nephrol 2008;3:1274-81.

149. Goo HW, Park IS, Ko JK, Kim YH, Seo DM, Park JJ. Computed tomography for the diagnosis of congenital heart disease in pediatric and adult patients. Int J Cardiovasc Imaging 2005;21:347-65.

150. Gartner RD, Sutton NJ, Weinstein S, Spindola-Franco H, Haramati LB. MRI and computed tomography of cardiac and pulmonary complications of tetralogy of Fallot in adults. J Thorac Imaging 2010;25:183-90.

151. Holzer RJ, Gauvreau K, Kreutzer J, Leahy R, Murphy J, Lock JE, et al. Balloon angioplasty and stenting of branch pulmonary arteries: adverse events and procedural characteristics: results of a multi-institutional registry. Circ Cardiovasc Interv 2011;4:287-96.

152. Juergens KU, Grude M, Maintz D, Fallenberg EM, Wichter T, Heindel W, et al. Multi-detector row CT of left ventricular function with dedicated analysis software versus MR imaging: initial experience. Radiology 2004;230:403-10.

153. Lembcke A, Dohmen PM, Dewey M, Klessen C, Elgeti T, Hermann KG, et al. Multislice computed tomography for preoperative evaluation of right ventricular volumes and function: comparison with magnetic resonance imaging. Ann Thorac Surg 2005;79:1344-51.

154. Raman SV, Shah M, McCarthy B, Garcia A, Ferketich AK. Multi-detector row cardiac computed tomography accurately quantifies right and left ventricular size and function compared with cardiac magnetic resonance. Am Heart J 2006;151:736-44.

155. Chung JH, Ghoshhajra BB, Rojas CA, Dave BR, Abbara S. CT angiography of the thoracic aorta. Radiol Clin North Am 2010;48:249-64.

156. Rathi VK, Doyle M, Williams RB, Yamrozik J, Shannon RP, Biederman RW. Massive aortic aneurysm and dissection in repaired tetralogy of Fallot; diagnosis by cardiovascular magnetic resonance imaging. Int J Cardiol 2005;101:169-70.

157. Kim WH, Seo JW, Kim SJ, Song J, Lee J, Na CY. Aortic dissection late after repair of tetralogy of Fallot. Int J Cardiol 2005;101:515-6.

158. Lu TL, Huber CH, Rizzo E, Dehmeshki J, von Segesser LK, Qanadli SD. Ascending aorta measurements as assessed by ECG-gated multi-detector

computed tomography: a pilot study to establish normative values for transcatheter therapies. Eur Radiol 2009;19:664-9.

159. Mao SS, Ahmadi N, Shah B, Beckmann D, Chen A, Ngo L, et al. Normal thoracic aorta diameter on cardiac computed tomography in healthy asymptomatic adults: impact of age and gender. Acad Radiol 2008;15: 827-34.

160. Hadamitzky M, Distler R, Meyer T, Hein F, Kastrati A, Martinoff S, et al. Prognostic value of coronary computed tomographic angiography in comparison with calcium scoring and clinical risk scores. Circ Cardiovasc Imaging 2011;4:16-23.

161. de Graaf FR, Schuijf JD, Delgado V, van Velzen JE, Kroft LJ, de Roos A, et al. Clinical application of CT coronary angiography: state of the art. Heart Lung Circ 2010;19:107-16.

162. Hamirani YS, Isma'eel H, Larijani V, Drury P, Lim W, Bevinal M, et al. The diagnostic accuracy of 64-detector cardiac computed tomography compared with stress nuclear imaging in patients undergoing invasive cardiac catheterization. J Comput Assist Tomogr 2010;34:645-51.

163. Hamdan A, Asbach P, Wellnhofer E, Klein C, Gebker R, Kelle S, et al. A prospective study for comparison of MR and CT imaging for detection of coronary artery stenosis. JACC Cardiovasc Imaging 2011;4:50-61.

164. Cook SC, Raman SV. Unique application of multislice computed tomography in adults with congenital heart disease. Int J Cardiol 2007;119:101-6.

165. Jakobs TF, Becker CR, Ohnesorge B, Flohr T, Suess C, Schoepf UJ, et al. Multislice helical CT of the heart with retrospective ECG gating: reduction of radiation exposure by ECG-controlled tube current modulation. Eur Radiol 2002;12:1081-6.

166. Pruckmayer M, Zacherl S, Salzer-Muhar U, Schlemmer M, Leitha T. Scintigraphic assessment of pulmonary and whole-body blood flow patterns after surgical intervention in congenital heart disease. J Nucl Med 1999; 40:1477-83.

167. Bourque JM, Beller GA. Stress myocardial perfusion imaging for assessing prognosis: an update. JACC Cardiovasc Imaging 2011;4:1305-19.

168. O'Laughlin MP, Slack MC, Grifka RG, Perry SB, Lock JE, Mullins CE. Implantation and intermediate-term follow-up of stents in congenital heart disease. Circulation 1993;88:605-14.

169. Jonsson H, Ivert T, Jonasson R, Wahlgren H, Holmgren A, Bjork VO. Pulmonary function thirteen to twenty-six years after repair of tetralogy of Fallot. J Thorac Cardiovasc Surg 1994;108:1002-9.

170. Wu MT, Huang YL, Hsieh KS, Huang JT, Peng NJ, Pan JY, et al. Influence of pulmonary regurgitation inequality on differential perfusion of the lungs in tetralogy of Fallot after repair: a phase-contrast magnetic resonance imaging and perfusion scintigraphy study. J Am Coll Cardiol 2007;49:1880-6.

171. Tamir A, Melloul M, Berant M, Horev G, Lubin E, Blieden LC, et al. Lung perfusion scans in patients with congenital heart defects. J Am Coll Cardiol 1992;19:383-8.

172. Boothroyd AE, McDonald EA, Carty H. Lung perfusion scintigraphy in patients with congenital heart disease: sensitivity and important pitfalls. Nucl Med Commun 1996;17:33-9.

173. Hashimoto K, Nakamura Y, Matsui M, Kurosawa H, Arai T. Alteration of pulmonary blood flow in tetralogy of Fallot: pre- and postoperative study with macroaggregates of ^{99m}Tc-labeled human serum albumin. Jpn Circ J 1992;56:992-7.

174. Dowdle SC, Human DG, Mann MD. Pulmonary ventilation and perfusion abnormalities and ventilation perfusion imbalance in children with pulmonary atresia or extreme tetralogy of Fallot. J Nucl Med 1990;31: 1276-9.

175. Reduto LA, Berger HJ, Johnstone DE, Hellenbrand W, Wackers FJ, Whittemore R, et al. Radionuclide assessment of right and left ventricular exercise reserve after total correction of tetralogy of Fallot. Am J Cardiol 1980;45:1013-8.

176. Hurwitz RA, Treves S, Kuruc A. Right ventricular and left ventricular ejection fraction in pediatric patients with normal hearts: first-pass radionuclide angiocardiography. Am Heart J 1984;107:726-32.

177. Manno BV, Iskandrian AS, Hakki AH. Right ventricular function: methodologic and clinical considerations in noninvasive scintigraphic assessment. J Am Coll Cardiol 1984;3:1072-81.

178. Cusimano RJ, Guest C. Coronary artery disease following repair of tetralogy of Fallot: implications and management. Can J Cardiol 1996;12:172-4.

179. Parker JA, Coleman RE, Grady E, Royal HD, Siegel BA, Stabin MG, et al. SNM practice guideline for lung scintigraphy 4.0. J Nucl Med Technol 2012;40:57-65.

180. Strauss HW, Miller DD, Wittry MD, Cerqueira MD, Garcia EV, Iskandrian AS, et al. Procedure guideline for myocardial perfusion imaging 3.3. J Nucl Med Technol 2008;36:155-61.

181. Bonhoeffer P, Boudjemline Y, Saliba Z, Merckx J, Aggoun Y, Bonnet D, et al. Percutaneous replacement of pulmonary valve in a right-ventricle to pulmonary-artery prosthetic conduit with valve dysfunction. Lancet 2000;356:1403-5.

182. McElhinney DB, Hellenbrand WE, Zahn EM, Jones TK, Cheatham JP, Lock JE, et al. Short- and medium-term outcomes after transcatheter pulmonary valve placement in the expanded multicenter us melody valve trial. Circulation 2010;122:507-16.

183. Geva T, Bergersen L, Kreutzer J. Diagnostic pathways for evaluation of congenital heart disease. In: Crawford MH, DiMarco JP, Paulus WJ, editors. Cardiology. Philadelphia: Elsevier; 2009. pp. 1415-40.

184. Noble S, Miro J, Yong G, Bonan R, Tardif JC, Ibrahim R. Rapid pacing rotational angiography with three-dimensional reconstruction: use and benefits in structural heart disease interventions. Eurointervention 2009;5: 244-9.

185. Glatz AC, Zhu X, Gillespie MJ, Hanna BD, Rome JJ. Use of angiographic CT imaging in the cardiac catheterization laboratory for congenital heart disease. JACC Cardiovasc Imaging 2010;3:1149-57.

186. Fagan T, Kay J, Carroll J, Neubauer A. 3-D guidance of complex pulmonary artery stent placement using reconstructed rotational angiography with live overlay. Catheter Cardiovasc Interv 2012;79:414-21.

187. Lock JE, Keane JF, Fellows KE. Diagnostic and interventional cardiac catheterization in congenital heart disease. Boston, MA: Martinus Nijhoff; 1987.

188. Chung T, Burrows PE. Diagnostic and interventional cardiac catheterization in congenital heart disease. Amsterdam, The Netherlands: Kluwer Academic; 2000.

189. Lock JE, Keane JF, Perry SB. Diagnostic and interventional cardiac catheterization in congenital heart disease. Amsterdam, The Netherlands: Kluwer Academic; 2000.

190. Zahn EM, Hellenbrand WE, Lock JE, McElhinney DB. Implantation of the melody transcatheter pulmonary valve in patients with a dysfunctional right ventricular outflow tract conduit early results from the U.S. clinical trial. J Am Coll Cardiol 2009;54:1722-9.

191. Alfakih K, Plein S, Thiele H, Jones T, Ridgway JP, Sivananthan MU. Normal human left and right ventricular dimensions for MRI as assessed by turbo gradient echo and steady-state free precession imaging sequences. J Magn Reson Imaging 2003;17:323-9.

192. Hudsmith LE, Petersen SE, Francis JM, Robson MD, Neubauer S. Normal human left and right ventricular and left atrial dimensions using steady state free precession magnetic resonance imaging. J Cardiovasc Magn Reson 2005;7:775-82.

193. Sarikouch S, Koerperich H, Boethig D, Peters B, Lotz J, Gutberlet M, et al. Reference values for atrial size and function in children and young adults by cardiac MR: a study of the German Competence Network congenital heart defects. J Magn Reson Imaging 2011;33:1028-39.

194. Robbers-Visser D, Boersma E, Helbing WA. Normal biventricular function, volumes, and mass in children aged 8 to 17 years. J Magn Reson Imaging 2009;29:552-9.

195. Buechel EV, Kaiser T, Jackson C, Schmitz A, Kellenberger CJ. Normal right- and left ventricular volumes and myocardial mass in children measured by steady state free precession cardiovascular magnetic resonance. J Cardiovasc Magn Reson 2009;11:19.